Towards atomistic resolution structure of phosphatidylcholine headgroup and glycerol backbone at different ambient conditions†

Alexandru Botan,[‡] Fernando Favela-Rosales,[¶] Patrick F. J. Fuchs,[§] Matti Javanainen,[‖] Matej Kanduč,[⊥] Waldemar Kulig,[‖] Antti Lamberg,[#] Claire Loison,[‡] Alexander Lyubartsev,[@] Markus S. Miettinen,[⊥] Luca Monticelli,[△] Jukka Määttä,[▽] O. H. Samuli Ollila,[*,▽] Marius Retegan,[††] Tomasz Rog,[‖] Hubert Santuz,[‡‡,¶¶,§§,‖‖] and Joona Tynkkynen[‖]

Institut Lumière Matière, UMR5306 Université Lyon 1-CNRS, Université de Lyon 69622 Villeurbanne, France, Departamento de Física, Centro de Investigación y de Estudios Avanzados del IPN, Apartado Postal 14-740, 07000 México D.F., México, Institut Jacques Monod, CNRS, Université Paris Diderot, Sorbonne Paris Cité, Paris, France, Department of Physics, Tampere University of Technology, Tampere, Finland, Fachbereich Physik, Freie Universitat Berlin, Berlin, Germany, Department of Chemical Engineering, Kyoto University, Kyoto, Japan, Division of Physical Chemistry, Department of Materials and Environmental Chemistry, Stockholm University, S-106 91 Stockholm, SWEDEN, Institut de Biologie et Chimie des Protéines (IBCP), CNRS UMR 5086, Lyon, France, Aalto University, Espoo, Finland, Max Planck Institute for Chemical Energy Conversion, Mulheim an der Ruhr, Germany, INSERM, UMR_S 1134, DSIMB, Paris, France, Université Paris Diderot, Sorbonne Paris Cité, UMR_S 1134, Paris, France, Institut National de la Transfusion Sanguine (INTS), Paris, France, and Laboratoire d'Excellence GR-Ex, Paris, France

E-mail: samuli.ollila@aalto.fi.

Abstract

Phospholipids are essential building blocks of biological membranes. Despite of vast amount of very accurate experimental data, the atomistic resolution structures sampled by the glycerol backbone and choline headgroup in phoshatidylcholine bilayers are not known. Atomistic resolution molecular dynamics simulations have the potential to resolve the structures, and to give an arrestingly intuitive interpretation of the experimental data—but only if the simulations reproduce the data within experimental accuracy. In the present work, we simulated phosphatidylcholine (PC) lipid bilayers with 13 different atomistic models, and compared simulations with NMR experiments in terms of the highly structurally sensitive C–H bond vector order parameters. Focusing on the glycerol backbone and choline headgroups, we showed that the order parameter comparison can be used to judge the atomistic resolution structural accuracy of the models. Accurate models, in turn, allow molecular dynamics simulations to be used as an interpretation tool that translates these NMR data into a dynamic three dimensional representation of biomolecules in biologically relevant conditions. In addition to lipid bilayers in fully hydrated conditions, we reviewed previous experimental data for dehydrated bilayers and cholesterol-containing bilayers, and interpreted them with simulations. Although none of the existing models reached experimental accuracy, by critically comparing them we were able to distill relevant chemical information: (1) increase of choline order parameters indicates the P–N vector tilting more parallel to the membrane, and

[†]Publication about results presented in the NMRlipids project
[*]To whom correspondence should be addressed
[‡]Lyon CNRS
[¶]Mexico
[§]CNRS Paris
[‖]Tampere University of Technology
[⊥]Freie Universität Berlin
[#]Kyoto University
[@]Stockholm University
[△]IBCP
[▽]Aalto University
[††]Max Planck
[‡‡]INSERM
[¶¶]Diderot
[§§]INTS
[‖‖]Labex

(2) cholesterol induces only minor changes to the PC (glycerol backbone) structure. This work has been done as a fully open collaboration, using `nmrlipids.blogspot.fi` as a communication platform; all the scientific contributions were made publicly on this blog. During the open research process, the repository holding our simulation trajectories and files (`https://zenodo.org/collection/user-nmrlipids`) has become the most extensive publicly available collection of molecular dynamics simulation trajectories of lipid bilayers.

Introduction

Phospholipids containing various polar headgroups and acyl chains are essential building blocks of biological membranes. Lamellar phospholipid bilayer structures have been widely studied with various experimental and theoretical techniques as a simple model for cellular membranes.[1–8] Phospholipid molecules are composed of hydrophobic acyl chains connected by a glycerol backbone to a hydrophilic headgroup; see Fig. 1 for the structure of 1-palmitoyl-2-oleoylphosphatidylcholine (POPC). The behaviour of the acyl chains in a lipid bilayer is relatively well understood.[1–5,8,9] The conformations sampled by the glycerol backbone and choline in a fluid bilayer are, however, not fully resolved as even the most accurate scattering and Nuclear Magnetic Resonance (NMR) techniques give only a set of values that the structure has to fulfill, but there is no unique way to derive the actual structure from them.[9–18] Some structural details have been extracted from crystal structures, ^{1}H NMR studies, and Raman spectroscopy,[19–25] but general consensus concerning the structures sampled in the fluid state has not been reached.[9–18,24,25] Importantly, the structural parameters for the glycerol backbone are similar for various biologically relevant lipid species (phosphatidylcholine (PC), phosphatidylethanolamine (PE) and phosphatidylglycerol (PG)) in various environments,[26] and the structural parameters for the choline headgroup are similar in model membranes and real cells (mouse fibroblast L-M cell).[27] Thus, resolving the PC-lipid glycerol and choline structures would be useful for understanding a wide range of

different biological membranes.

Classical atomistic molecular dynamics simulations have been widely used to study lipid bilayers.[2–7] As these models provide an atomistic resolution description of the whole lipid molecule, they have the potential to solve the glycerol backbone and headgroup structures. The experimental C–H bond order parameters (routinely compared between experiments and simulations for the acyl chains[2–6]) are also known for the glycerol backbone (g_1, g_2, and g_3) and choline (α and β) segments (see Fig. 1 for definitions) and are among the main parameters used in attempts to derive lipid structures from experimental data.[10–13,15,16,18] Notably, the structures sampled in a simulation that reproduces these parameters will automatically comprise an interpretation of the experiments. In other words, such simulations can be considered as an accurate atomistic resolution description of the behavior of lipid molecules in a bilayer.

Only a few studies[28–37] have compared the glycerol backbone and choline headgroup order parameters between simulations and experiments. The main reason probably is that the existing experimental data for the glycerol backbone and choline headgroups are scattered over many publications and published in a format that is difficult to understand without some NMR expertise. In addition to the order parameters, dihedral angles for the glycerol backbone and headgroup estimated from experiments have sometimes been used to assess the quality of a simulation model.[28,38–42]

In this work, we first review the most relevant experimental data for the glycerol backbone and choline headgroup order parameters in a phosphatidylcholine lipid bilayer. Then the available atomistic resolution lipid models are carefully compared to the experimental data. The comparison reveals that the CHARMM36,[31] GAFFlipid,[33] and MacRog[37] models have the most realistic glycerol backbone and choline structures. We also compare the glycerol backbone and choline structures between the most often used (Berger-based) lipid model[43] and the best performing models, to demonstrate that by using the order parameters we can distinguish the more reasonable structures from the less reasonable ones. However, none of

the current models is accurate enough to properly resolve the atomistic resolution structures.

In addition to fully hydrated single component lipid bilayers, the glycerol backbone and choline order parameters have been measured under a large number of changing conditions: hydration level,[44–46] cholesterol content,[35,47] ion concentration,[48–52] temperature,[53] charged lipid content,[51,52] charged surfactant content,[54] drug molecule concentration,[30,55,56] and protein content[57,58] (listing only the publications most relevant for this work and the pioneering studies). Existence of these data allows the comparison of structural responses to varying conditions between simulations and experiments, in other words, validation of the simulation models and interpretation of the original experiments. Here we demonstrate the power of this approach in understanding the behaviour of a bilayer as a function of hydration level and cholesterol content. Choline headgroup order parameters as function of ion concentration, and their relation to the ion binding affinity, are discussed elsewhere.[59]

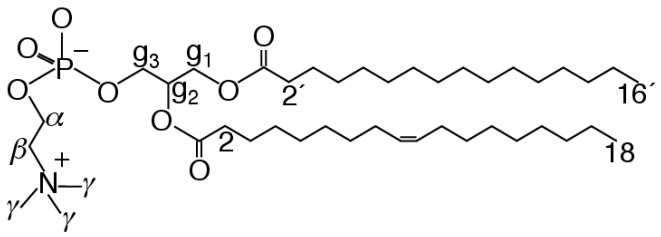

Figure 1: Chemical structure of 1-palmitoyl-2-oleoylphosphatidylcholine (POPC).

Methods

Open collaboration

This work has been done as a fully open collaboration, using the `nmrlipids.blogspot.fi` blog[60] as a communication platform. Our approach is inspired by the Polymath project,[61] however there are some essential differences. We started by publishing a manuscript[62] discussing the glycerol backbone and choline structures in a Berger-based model (the most used molecular dynamics simulation model for lipid bilayers). Simultaneously, we presented an open invitation for further contributions and discussion on the blog. All the scientific contributions were made publicly through the blog. Every contributor was offered coauthorship according to the guidelines defined in the beginning of the project;[63] the acceptance of the offer was based on authors' self-assesment of their scientific contribution. These contributions are summarized in the Supplementary Information.

Almost all simulation data, including input files for reproduction and trajectories for further analysis, are collected on our CERN-hosted Zenodo file repository (`https://zenodo.org/collection/user-nmrlipids`). Thus, in addition to the main topic of this manuscript, we present the most extensive publicly available collection of simulation trajectories for lipid bilayers, opening up numerous possiblities for different analyses with much less effort than previously required. Further information, such as scripts, figures, and manuscript text files, are available through our GitHub repository (`https://github.com/NMRlipids`). **1.I will not assign a doi yet. We can wait for the journal decision.**.

Order parameters from experiments

The order parameter of a hydrocarbon C–H vector is defined as

$$S_{\mathrm{CH}} = \frac{1}{2}\langle 3\cos^2\theta - 1\rangle, \tag{1}$$

where the angle brackets denote an ensemble average over the sampled conformations, and θ is the angle between the C–H bond and the membrane normal. The absolute values of order parameters can be measured by detecting quadrupolar splitting with ^{2}H NMR[64] or by detecting dipolar splitting with ^{1}H-^{13}C NMR.[35,65–67] The measurements are based on different physical interactions and also the connection between order parameters and quadrupolar or dipolar splitting are different. The absolute values of order parameters from the measured quadrupolar splitting $\Delta\nu_Q$ (^{2}H NMR) are calculated using the equation $|S_{\mathrm{CD}}| = \frac{4}{3}\frac{e^2qQ}{h}\Delta\nu_Q$, where the value for the static quadrupole splitting constant is estimated from various experiments to be 170 kHz leading to a numerical relation $|S_{\mathrm{CD}}| = 0.00784 \times \Delta\nu_Q$.[64] The absolute values of order parameters from the effective dipolar coupling d_{CH} (^{1}H-^{13}C NMR) are calculated using equation $|S_{\mathrm{CH}}| = \frac{4\pi\langle r_{\mathrm{CH}}^3\rangle}{\hbar\mu_0\gamma_h\gamma_c}d_{\mathrm{CH}}$, where values between 20.2–22.7 kHz are used for $\frac{4\pi\langle r_{\mathrm{CH}}^3\rangle}{\hbar\mu_0\gamma_h\gamma_c}$, depending on the original authors.[35,65–67] The effective dipolar coupling d_{CH} is related to the measured dipolar splitting $\Delta\nu_{CH}$ through scaling factor which depends on the pulse sequence used in the ^{1}H-^{13}C NMR experiment.[35,65–67] It is important to note that the order parameters measured with different techniques based on different physical interactions are in good agreement with each other (see Results and Discussion), indicating very high quantitative accuracy of the measurements. For a more detailed discussion see Ref. 68.

The absolute values of order parameters are accessible with both ^{2}H NMR and ^{1}H-^{13}C NMR techniques. However, only ^{1}H-^{13}C NMR techniques allow also the measurement of the sign of the order parameter.[16,65,66] The measured sign is negative for almost all the carbons discussed in this work, except for α which is positive.[16,65,66] For more detailed discussion about the determination of the sign of the order parameters see Ref. 69.

For most CH_2 segments in fluid phosholipid bilayer the order parameters are equal for both hydrogens attached to the same carbon. However, in some cases (e.g. g_1, g_3 and C_2 carbon in the *sn*-2 chain) the order parameters are not equal and this can be observed with both ^{2}H NMR and ^{1}H-^{13}C NMR techniques. In the present work we call the phenomena

of unequal order parameters for hydrogens attached to the same carbon as *forking* to avoid confusion with dipolar and quadrupolar splitting in NMR terminology. Forking has been studied in detail with ^{2}H NMR techniques by deuterating the R or S position in CH_2 segment, and the studies show that the forking arises from differently sampled orientations of the two C–H bonds, not from two separate populations of lipid conformations.[26,70]

Order parameters from simulations

The order parameters from simulations were calculated directly using the definition as in Eq. 1. For the united atom models the hydrogen positions were generated in the trajectories post-simulationally using the positions of the heavy atoms and the known hydrocarbon geometries. For the statistical error estimates, the time average of order parameters were first calculated separately for each lipid in the system. Then it was assumed that different lipids are statistically independent entities (which should be the case in fluid phase) and the error of the mean for the average over individual lipids in the system was calculated and used as error bar for the order parameters.

It has been recently pointed out that the sampling of individual dihedral angles might be very slow compared to the typical simulation timescales.[71] On the other hand, another recent study shows that the slowest rotational correlation functions of a C–H bond (g_1) reaches a plateau (S^2_{CH}) after 200 ns in the Berger-POPC-07[72] model, and that the dynamics of this segment is significantly too slow in simulations compared to the experiments.[73] In practise, less than 200 ns of simulation data is enough for the order parameter calculation due to the average over different lipid molecules. In conclusion, if the sampling with typical simulation times is not enough for the convergence of the order parameters, then the simulation models has significantly too slow dynamics.

Simulated systems

All simulations are ran with a standard setup for a planar lipid bilayer in zero tension and constant temperature with periodic boundary conditions in all directions by using the GROMACS software package[74] (version numbers 4.5.X–4.6.X), LAMMPS,[75] MDynaMix[76] or NAMD.[77] The number of molecules, simulation temperatures and the length of simulations of all the simulated systems are listed in Tables 1, 2 and 3. Full simulation details are given in the Supplementary Information (SI) or in the original publications in case the data is used previously therein. Additionally, the files related to the simulations and the resulting trajectories are publicly available for almost all systems in the Zenodo collection `https://zenodo.org/collection/user-nmrlipids`. The references pointing to simulation details and files are also listed in Tables 1, 2 and 3.

Results and Discussion

Full hydration: Experimental order parameters for the glycerol backbone and headgroup

The specific deuteration of α-, β- and g_3- segments of DPPC has been successful, allowing the absolute value order parameter measurements for these segments by ^{2}H NMR.[47–49,53] In addition, the absolute values of order parameters for all glycerol backbone and choline headgroup segments in egg yolk lecithin,[65] DMPC,[16,66,67] DOPC[139] and POPC[35,139] have been measured with several different implementations of ^{1}H-^{13}C NMR experiments. In addition, the signs of order parameters in some systems are measured with ^{1}H-^{13}C NMR techniques.[16,65,66] The experimental values of glycerol backbone and choline order parameters from various publications[35,49,53,66,67] with the signs measured in[16,65,66] are shown in Fig. 2.

In general there is a good agreement between the order parameters measured with different experimental NMR techniques: Almost all the reported values are within a variation

Table 1: Fully hydrated single component lipid bilayer systems simulated for Fig. 2: 1,2-dimyristoyl-sn-glycero-3-phosphocholine (DMPC), dilauroylphosphatidylcholine (DLPC), dipalmitoylphosphatidylcholine (DPPC), and 1-palmitoyl-2-oleoylphosphatidylcholine (POPC). The **bolded** systems were used also for Fig. 3. [a] Number of lipid molecules. [b] Number of water molecules. [c] Temperature. [d] Total simulation time. [e] Time used for analysis. [f] Reference link for the downloadable simulation files; the data sets marked with * also include a part of the trajectory. [g] Reference for the full simulation details; the original publication is cited if simulation data from previously published work has been directly used, for other systems the simulation details are given in the Supplementary Information. [h] Magnitudes from Fig. S4 of Klauda et al.,[31] signs matched to our simulations. [i] Magnitudes from Fig. 9 of Dickson et al.,[33] signs matched to our simulations.

Force field	lipid	[a]N_l	[b]N_w	[c]T (K)	[d]t_{sim}(ns)	[e]t_{anal} (ns)	[f]Files	[g]Details
Berger-DMPC-04[78]	DMPC	128	5097	323	130	100	[79]*	[80]
Berger-DPPC-98[81]	DPPC	72	2864	323	60	30	[82]*	SI
Berger-POPC-07[72]	POPC	128	7290	298	270	240	[83]*	[73]
CHARMM36[31]	DPPC	72	2189	323	30	25	[84]*	SI
CHARMM36[31]	DPPC	72	2189	323	130	-	-	[31][h]
CHARMM36[31]	POPC	72	2242	303	30	20	[85]*	SI
CHARMM36[31]	POPC	128	5120	303	200	100	[86]*	SI
MacRog[87]	POPC	288	12600	310	100	80	[88]*	SI
MacRog[87]	POPC	128	6400	310	400	200	[89]*	SI
MacRog[87]	POPC	288	14400	310	90	40	[90]*	SI
GAFFlipid[33]	DPPC	72	2197	323	90	50	[91]*	SI
GAFFlipid[33]	DPPC	72	2167	323	250	250	-	[33][i]
GAFFlipid[33]	POPC	126	3948	303	137	32	[92]*	SI
Lipid14[93]	POPC	72	2234	303	100	50	[94]*	SI
Poger[95]	DPPC	128	5841	323	2×100	2×50	[96,97]*	SI
Slipids[98]	DPPC	128	3840	323	150	100	[99]*	SI
Slipids[100]	POPC	128	5120	303	200	150	[101]*	SI
Kukol[102]	POPC	512	20564	298	50	30	[103]*	SI
Chiu[104]	POPC	128	3552	298	56	50	[105]*	SI
Högberg08[29]	DMPC	98	3840	303	75	50	[106]*	[29]
Högberg08[107]	POPC	128	3840	303	100	80	[108]*	[107]
Ulmschneiders[109]	POPC	128	3328	310	100	50	[110]*	SI
Tjörnhammar14[111]	DPPC	144	7056	323	200	100	[112]*	[111]
Botan-CHARMM36-UA[113]	DLPC	128	3840	323	30	20	[114]	SI
Lee-CHARMM36-UA[115]	DPPC	72	2189	323	70	50	[116]*	SI

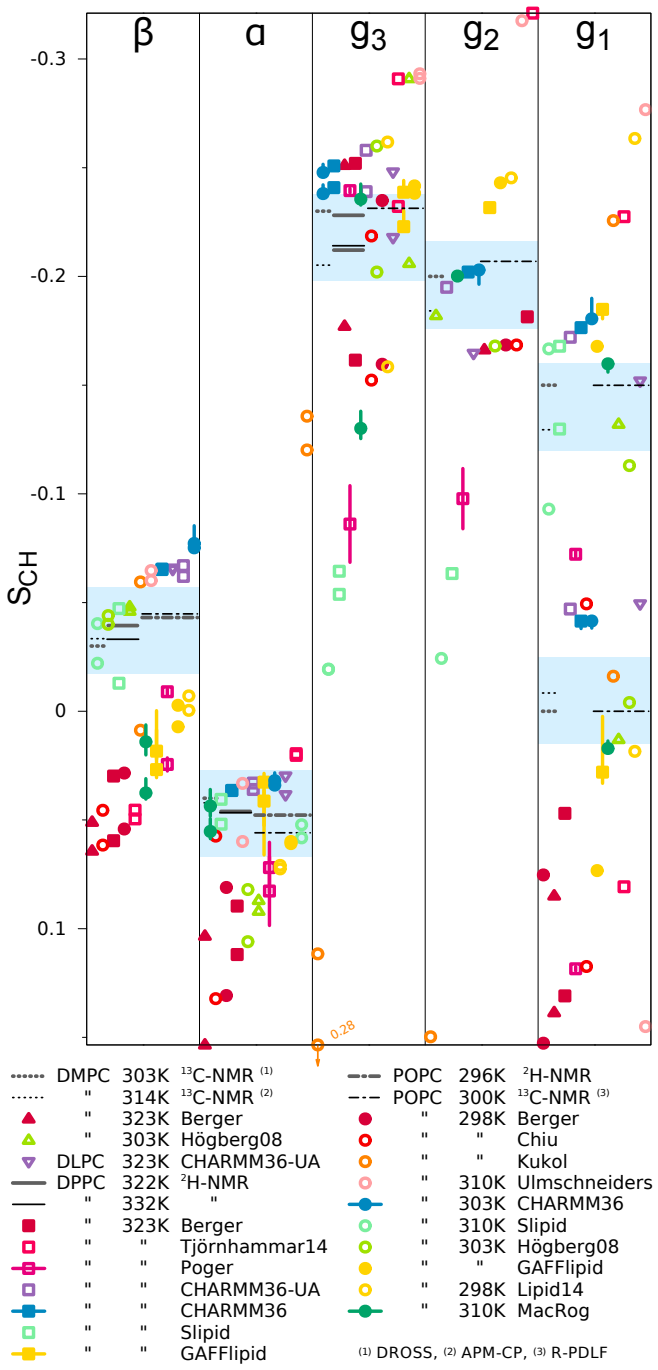

Figure 2: Order parameteres from simulations listed in Table 1 and experiments for glycerol and choline groups. The experimental values were taken from the following publications: DMPC 303 K from,[66] DMPC 314 K from,[67] DPPC 322 K from,[53] DPPC 323 K from,[49] POPC 296 K from,[44] and POPC 300 K from.[35] The vertical bars shown for some of the computational values are not error bars, but demonstrate that for these systems we had at least two data sets (see Table 1); the ends of the bars mark the extreme values from the sets, and the dot marks their measurement-time-weighted average. The interactive version of this figure is available at https://plot.ly/~HubertSantuz/72/lipid-force-field-comparison/.

Table 2: Simulated single component lipid bilayers with varying hydration levels. The simulation file data sets marked with * include also part of the trajectory. [a] Water/lipid molar ratio [b] The number of lipid molecules [c] The number of water molecules [d] Simulation temperature [e] The total simulation time [f] Time frames used in the analysis [g] Reference link for the downloadable simulation files [h] Reference for the full simulation details

Force field	lipid	[a]n (w/l)	[b]N_l	[c]N_w	[d]T (K)	[e]t_{sim}(ns)	[f]t_{anal} (ns)	[g]Files	[h]Details
Berger-POPC-07[72]	POPC	57	128	7290	298	270	240	[83]*	SI
	POPC	7	128	896	298	60	50	[117]*	SI
Berger-DLPC-13[118]	DLPC	28	72	2016	300	80	60	[119]*	[118]
	DLPC	24	72	1728	300	80	60	[120]*	[118]
	DLPC	20	72	1440	300	80	60	[121]*	[118]
	DLPC	16	72	1152	300	80	60	[122]*	[118]
	DLPC	12	72	864	300	80	60	[123]*	[118]
	DLPC	8	72	576	300	80	60	[124]*	[118]
	DLPC	4	72	288	300	80	60	[125]*	[118]
CHARMM36[31]	POPC	40	128	5120	303	150	100	[86]*	SI
	POPC	31	72	2242	303	30	20	[85]*	SI
	POPC	15	72	1080	303	59	40	[126]*	SI
	POPC	7	72	504	303	60	20	[127]*	SI
MacRog[87]	POPC	50	288	14400	310	90	40	[90]*	SI
	POPC	25	288	7200	310	100	50	[90]*	SI
	POPC	20	288	5760	310	100	50	[90]*	SI
	POPC	15	288	4320	310	100	50	[90]*	SI
	POPC	10	288	2880	310	100	50	[90]*	SI
	POPC	5	288	1440	310	100	50	[90]*	SI
GAFFlipid[33]	POPC	31	126	3948	303	137	32	[92]*	SI
	POPC	7	126	896	303	130	40	[128]*	SI

of ± 0.02 (which is also the error estimate given by Gross et al.[66]) for all fully hydrated PC bilayer, regardless of the variation in their acyl chain composition and temperature. Exceptions are the somewhat lower order parameters sometimes reported from measurements using ^{1}H-^{13}C NMR.[16,65,139] These experiments are not shown in Fig. 2 as the reported error bars are either relatively large,[16,65] or the spectral resolution is quite low and the numerical lineshape simulations have not been used in the analysis.[139] Due to this end, it is highly likely that these reported lower order parameters are due to lower experimental accuracy and therefore we exclude them from our discussion. For more details, see Ref. 68. Motivated by the high experimental reproducibility, we have highlighted in Fig. 2 the subjective sweet spots (light blue areas), within which we expect the calculated absolute values of the order

Table 3: Simulated lipid bilayers containing cholesterol. The simulation file data sets marked with * include also part of the trajectory. [a] The number of lipid molecules [b] The number of cholesterol molecules [c] Cholesterol concentration (mol%) [d] The number of water molecules [e] Simulation temperature [f] The total simulation time [g] Time frames used in the analysis [h] Reference link for the downloadable simulation files [i] Reference for the full simulation details

Force field	lipid	[a]N_l	[b]N_{chol}	[c]C_{CHOL}	[d]N_w	[e]T (K)	[f]t_{sim}(ns)	[g]t_{anal} (ns)	[h]Files	[i]Details
Berger-POPC-07[72] /Höltje-CHOL-13[35,129]	POPC	128	0	0%	7290	298	270	240	[83]*	[73]
	POPC	120	8	6%	7290	298	100	80	[130]*	[35]
	POPC	110	18	14%	8481	298	100	80	[131]*	[35]
	POPC	84	44	34%	6794	298	100	80	[132]*	[35]
	POPC	64	64	50%	10314	298	100	80	[133]*	[35]
	POPC	50	78	61%	5782	298	100	80	[134]*	[35]
CHARMM36[31,135]	POPC	128	0	0%	5120	303	150	100	[86]*	SI
	POPC	512	0	0%	23943	298	170	100	[136]*	SI
	POPC	460	52	10%	23569	298	170	100	[136]*	SI
	POPC	436	76	15%	23331	298	170	100	[136]*	SI
	POPC	100	24	19%	4960	303	200	100	[137]*	SI
	POPC	410	102	20%	20972	298	170	100	[136]*	SI
	POPC	384	128	25%	22327	298	170	100	[136]*	SI
	POPC	332	180	35%	21340	298	170	100	[136]*	SI
	POPC	256	256	50%	20334	298	170	100	[136]*	SI
	POPC	80	80	50%	4496	303	200	100	[138]*	SI
MacRog[87]	POPC	128	0	0%	6400	310	400	200	[89]*	SI
	POPC	114	14	11%	6400	310	400	200	[89]*	SI
	POPC	72	56	44%	6400	310	400	200	[89]*	SI
	POPC	64	64	50%	6400	310	400	200	[89]*	SI
	POPC	56	72	56%	6400	310	400	200	[89]*	SI

parameters of a well-performing force field to fall.

In addition to the numerical values, an important feature of the glycerol backbone is the forking (see section 1) of the order parameters in g_1 and g_3 segments, in contrast to the choline segments α and β. The forking in glycerol backbone g_3 segment is small (≈ 0.02) and some experiments only report the larger value or the average value.[35,49] In contrast, forking is significant for the glycerol backbone g_1 segment, whose lower order parameter is close to zero and the larger one has an absolute value of approximately 0.13–0.15. Forking was studied in detail by Gally et al.,[26] who used E. Coli to stereospecifically deuterate the different hydrogens attached to the g_1 or g_3 groups in PE lipids, and measured the order parameters from the lipid extract. This experiment gave the lower order parameter when deuterium was in the S position of g_1 or R position for g_3. Since the glycerol backbone order parameters are very similar irrespective of the headgroup chemistry (PC,PE and PG) or lipid environment,[26] it is reasonable to assume that the stereospecifity measured for the PE lipids holds also for the PC lipids.

The most detailed experimentally available order parameter information for the glycerol backbone and choline segments of POPC bilayer is collected by taking the absolute values from,[35] the signs from[16,65,66] and the stereospecific labeling from,[26] and shown in Fig. 3.

Full hydration: Comparison between simulation models and experiments

The order parameters of the glycerol backbone and headgroup calculated from different force fields for various lipids have been previously compared to experiments.[28–37] The general conclusion from these studies seems to be that the CHARMM based,[29,31] GAFFlipid[33] and MacRog[37] force fields perform better for the glycerol backbone and headgroup structures than the GROMOS based models.[30,32,34,35] However, none of the studies exploits the full potential of the available experimental data discussed in previous section, i.e. the quantitative accuracy, known signs and stereospecific labeling of the experimental order parameters.

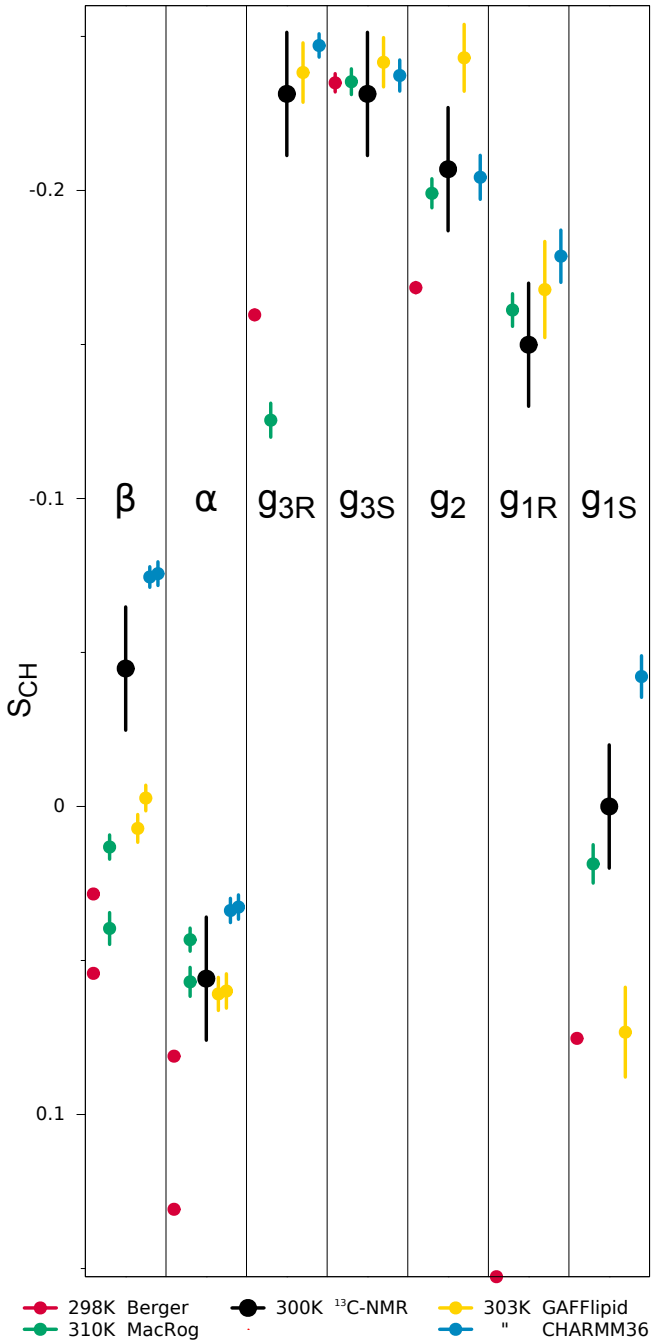

Figure 3: Order parameteres for POPC glycerol and choline groups from simulations with Berger-POPC-07, MacRog, GAFFlipid, and CHARMM36 force fields (the **bolded** systems in Table 1) together with experimental values. The error bars of simulation data are standard errors of mean (see Methods for details). The magnitudes for experimental order parameters are taken from Ferreira et al.,[35] the signs are based on the measurements by Hong et al.[16,65] and Gross et al.,[66] and the R/S labeling is based on the measurements by Gally et al.[26]

To get a general idea of the quality of the glycerol backbone and choline headgroup structures in different models, we calculated the order parameters for these parts from thirteen different lipid models (Table 1) and plotted the results together with experimental values in Fig. 2. Two criteria were used to judge the quality of the model: there must not be significant **forking** in the α and β carbons, there must be only moderate forking in the g_3 carbon and there must be significant forking in the g_1 carbon, the **magnitude** should be preferably inside to the subjective sweet spots determined from experiments (blue shaded regions in Fig. 2). The results for each force field in respect to the above criteria are summarized in Figure 4.

None of the studied force fields fulfils these criteria completely, however CHARMM36 is pretty close. This is not surprising since the dihedral potentials in this model are tuned to reproduce these parameters better against experiments.[31] The next models in the list are CHARMM36-UA[113,115] and Högberg08[29] which is also not surprising since these models are using CHARMM bonded potentials for glycerol backbone and choline. The fourth and the fifth models in the list, MacRog[37] and GAFFlipid,[33] have independently determined dihedral potentials. All the models based on Gromos potentials and Slipids perform less well. In the present work we subject the CHARMM36, MacRog, GAFFlipid and Berger-POPC-07 to a more careful comparison including the sterospecific labeling (Fig. 3), and atomistic level structure and responses to the dehydration and cholesterol content in the following sections. These models are selected for more detailed studies since they are the best representatives of different dihedral potential parametrization techniques (CHARMM36, MacRog, GAFFlipid), and the Berger based models are the most used lipid model in the literature.

Full hydration: Atomistic resolution structures in different models

The results in the previous section revealed significant differences of the glycerol backbone and choline headgroup order parameters between different molecular dynamics simulation models. However, it is not straightforward to conclude which kind of structural differences (if

Figure 4: Rough ranking of force fields based on data of Fig. 2. "M" indicates a magnitude problem, "F" a forking problem. Letter size shows the level (0-4) of severity; the Σ-column shows the sum of these, i.e., the "total severity". Color scheme: "within experimental error" (dark green), "almost within experimental error" (light green), "clear deviation from experiments" (light red), and "major deviation from experiments" (dark red).

any) between the models the results indicate, because the mapping from the order parameters to the structure is not unique. In this section we demonstrate that 1) the differences in order parameters indicate significantly different structural sampling strongly correlating with the dihedral angles of the related bonds, and that 2) the comparison between experimental and simulated order parameters can be used to exclude nonrealistic structural samping in molecular dynamics simulations. The demonstration is done for the dihedral angles defined by the g_3-g_2-g_1-O(sn-1) segments in the glycerol backbone and the N-β-α-O segments in the headgroup. These dihedrals were chosen for demonstration, because significant differences between the models are observed around these segments in Fig. 3. We note that performing a similar comparison through all the dihedrals in all the 13 models would probably give highly useful information on how to improve the accuracy of the models yet this is beyond the scope of the current report.

The dihedral angle distributions for the g_3-g_2-g_1-O(sn-1) dihedral calculated from different models are shown in Fig. 5. The distribution is qualitatively different for the Berger-POPC-07 model, showing a maximum in the gauche$^+$-conformation (60^o) compared to all the other models showing a maximum in the anti-conformation (180^o). The distributions in all the other models have the same general features, the main difference being that the fraction of configurations in the gauche$^-$-conformation (-60^o) is zero for the MacRog, detectable for the CHARMM36 and equally large to the gauche$^+$ fraction in GAFFlipid. From the results we conclude that most likely the wrongly sampled dihedral angle for the g_2-g_1 bond explains the significant discrepancy to the experimental order parameters for the g_1 segment in the Berger-POPC-07 model (Fig. 3). In conclusion, models preferring the anti conformation for this dihedral give more realistic order parameters and this is in agreement with previous crystal structure and ^{1}H NMR studies.[19–21,23–25]

The dihedral angle distribution for the N-β-α-O dihedral calculated from the same four models is shown in Fig. 6. Also for this dihedral there are significant differences in the gauche–anti fractions. The gauche conformations are dominant in the CHARMM36, in MacRog there

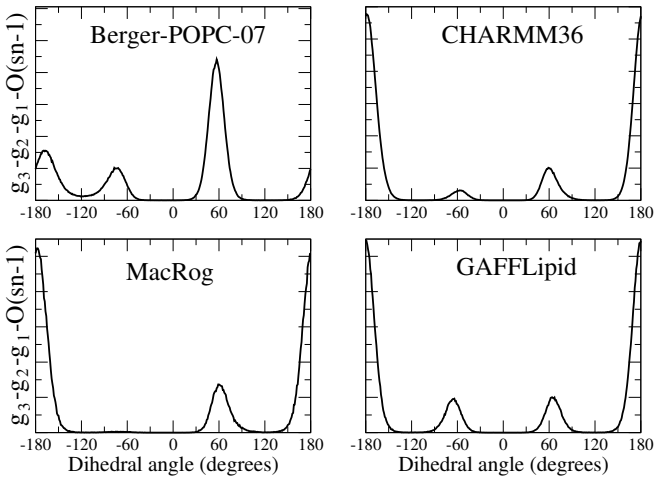

Figure 5: Dihedral angle distributions for g_3-g_2-g_1-O(sn-1) dihedral from different models (POPC bilayer in full hydration).

are only anti conformations present, and in the Berger-POPC-07 and GAFFlipid gauche and anti conformations have equal probabilities. On the other hand, comparison of α and β order parameters in Fig. 3 reveals that for these carbons the CHARMM36 is closest to the experimental results and it is also the only model that has the correct sign (negative) for the β order parameter. This result is again in agreement with previous crystal structure, ^{1}H NMR and Raman spectroscopy studies[19–22] which suggest that this dihedral is in the gauche conformation in the absence of ions.

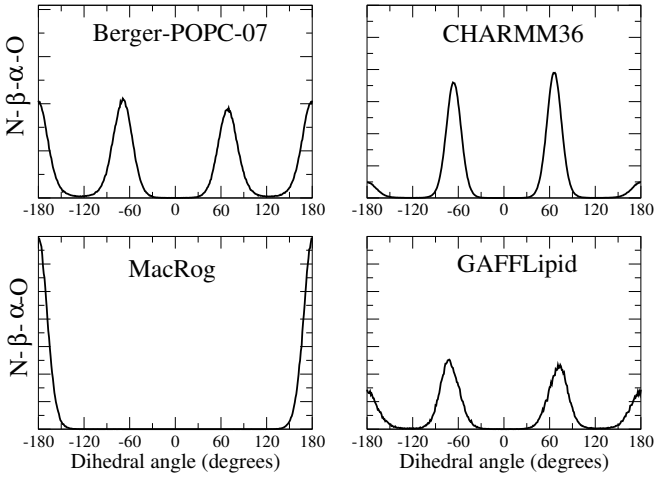

Figure 6: Dihedral angle distributions for N-β-α-O dihedral from different models (POPC bilayer in full hydration).

The used examples show that the glycerol backbone and headgroup order parameters reflect the atomistic resolution structure and that the comparison with experiments allows the assessment of the quality of the suggested structure. We were able to pinpoint specific problems in the structures in different models and suggest potential improvement strategies. If the improved atomistic molecular dynamics simulation model reproduced the order parameters and other experimental observables (like chemical shift anisotropy) with experimental accuracy, it would give an interpretation for the atomistic resolution structure of the glycerol backbone and choline.[10–13,15,16,18] The research along these lines is left, however, for future studies.

Response to dehydration and cholesterol content

In addition to pure phosphatidylcholine bilayers at full hydration, the choline headgroup order parameters have been measured under various different conditions.[30,32,35,44–50,53,54] Also the order parameters for the glycerol backbone have been measured with ^{1}H-^{13}C NMR in dehydrated conditions,[46] and as a function of anesthetics[30] and glycolipids[32] for DMPC, and as a function of cholesterol concentration for POPC.[35] Due to the high resolution in the NMR (especially ^{2}H NMR) experiments, even very small order parameter changes resulting from the varying conditions can be measured (see Ref. 68 for more discussion.) However, as already discussed above, it is not simple to deduce the structural changes from order parameter changes.[15,18] Consequently, comparison of the order parameters between simulations and experiments in different conditions can be used to assess the quality of the force field in different situations, and, if the quality is good, to interpret the structural changes in experiments. Here we exemplify such comparison for a lipid bilayer under low hydration levels and when varying amounts of cholesterol is included in the bilayer. The interaction between ions and a phosphatidylcholine bilayer will be discussed in a separate study.[59]

Phospholipid bilayer with low hydration level

Fig. 7 shows the published[44–46] experimental order parameters for the glycerol backbone and choline as a function of hydration level. Despite slight differences in temperature and acyl chain composition, the three independently reported data sets for the choline (β and α) segments agree well with each other: Both order parameters increase with decreasing hydration level. The glycerol backbone order parameters (g_3, g_2, g_1), in contrast, have been observed[46] to slightly decrease with dehydration. Note that the original experiments[44–46] measured only absolute values, but here we included the signs measured in separate studies.[16,65,66] Consequently, the negative β order parameter actually increases with dehydration as its absolute value decreases.[44–46]

Lipid bilayer dehydration has been studied also with molecular dynamics simulations,[140–145] typically motivated by the discussion concerning the origin of the "hydration repulsion".[146–148] Only one[140] of these studies, however, compared their simulation model to the experimental choline and glycerol backbone order parameters. Fig. 7 shows these order parameters as a function of hydration level for the CHARMM36, MacRog and GAFFlipid models (having the most realistic atomistic resolution structures) and a Berger-based model (which is the most used lipid model); note that the simulation results have been vertically shifted to ease the comparison with experimental response to dehydration. Despite of some fluctuations, the increase of the choline (β and α) order parameters is seen in all four models. The response of the choline order parameters to dehydration can, therefore, be interpreted to qualitatively agree with experiments. The situation is significantly more complicated for the glycerol backbone: None of the four models produced the experimentally seen trends in all the (g_3, g_2, g_1) segments.

The qualitative agreement of the α and β order parameters with experiments in all four simulation models (Fig. 7) indicates that, despite the unrealistic structures at full hydration (Figs. 2 and 4), the structural response of the choline headgroup to dehydration is somewhat realistic. A likely explanation is that as the interlamellar space shrinks with dehydration,

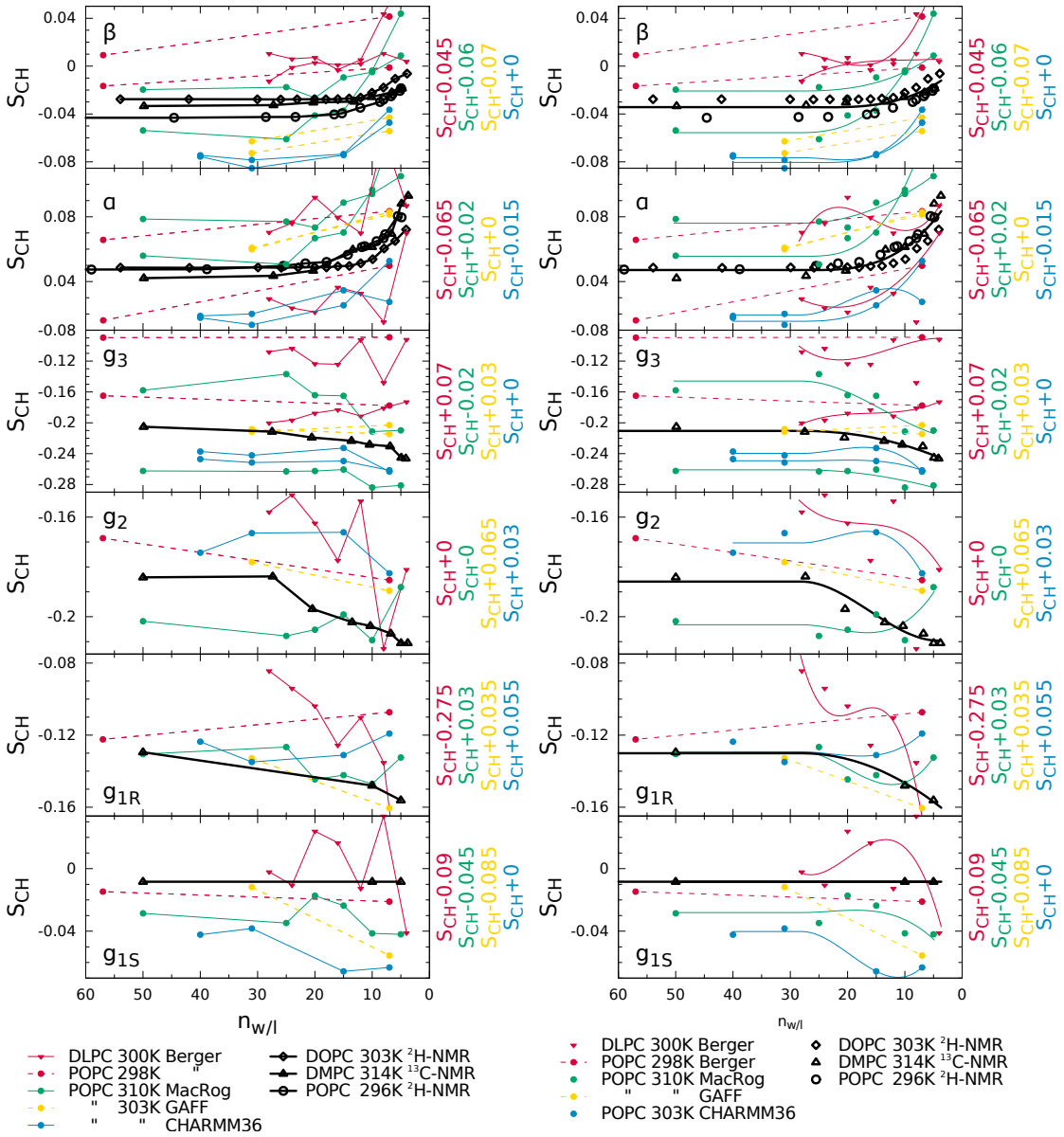

Figure 7: The effect of dehydration on glycerol and choline order parameters in experiments. The magnitudes of order parameters are measured for DMPC (^{1}H-^{13}C NMR) at 314 K,[46] for POPC (^{2}H NMR) at 296 K[44] and for DOPC (^{2}H NMR) at 303 K.[45] The signs are based on the measurements by Hong et al.[16,65] and Gross et al.[66] Note that to elucidate the relative change as a function of hydration level, the simulation results are shifted such that the (smaller) S_{CH} matches (within ± 0.01) the experimental value at full hydration; the shift magnitudes for each of the force fields are listed (S_{CH}+shift) in the y-label.

2.Markus prepared two versions of this plot. The one on left has all the data points joint by lines; the one on right shows smooth trend lines (cubic polynomials) to ease qualitative comparison. Samuli likes the one on left, Markus the one on right. Do others have opinions?

the whole choline group orients more parallel to the membrane. Indeed, upon dehydration the angle between P–N (phoshate phosphorus to choline nitrogen) vector and membrane normal increases for all the four models (Fig. 8). However, the amount of increase depends on the model. Especially the DLPC simulations with Berger model predict significantly stronger P–N vector tilt than the other models. The Berger model has also generally larger P–N vector angles and its choline order parameters are more off from experiments than the other three models (Fig. 3). Thus the relatively modest tilting with dehydration predicted by MacRog, CHARMM36 and GAFFlipid is probably more realistic.

It must be stressed that in the models incapable of reproducing the experimental order parameters the free energy landscape is not correct. Thus even though the order parameter response to dehydration is qualitatively correct, the energetic response is likely to be incorrect. This may have some influence on dehydration energetic calculations made using the Berger model.[143,145]

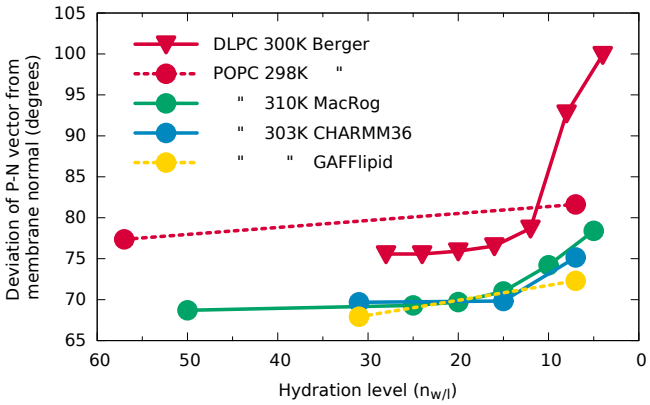

Figure 8: The average angle between membrane normal and P–N vector as function of hydration level calculated from different simulations.

The response of the glycerol backbone seems to be more subtle than that of the choline headgroup; none of the four models reproduced the experimental trends upon dehydration with enough accuracy to invite a structural interpretation.

Cholesterol-containing phospholipid bilayer

As cholesterol is abundant in biological membranes and has been suggested to be an important player, for example, in domain formation,[154,155] phospholipid–cholesterol interactions have been extensively studied with theoretical[149–152] and experimental[8,35,47,153] methods. It is widely agreed that cholesterol orders lipid acyl tails and thus decreases the area per molecule (condensing effect), but its influence on the lipid headgroup and glycerol backbone remains debated.[149,154,155] It has been suggested, for example, that the surrounding phospholipids shield cholesterol from exposure to water by reorienting their headgroups ("umbrella model")[149] or that cholesterol acts as a spacer between the headgroups to increase their entropy and dynamics ("superlattice model").[155] Molecular dynamics simulations have supported both the umbrella[152] as well as the superlattice[150] model, in addition to suggesting specific interactions of cholesterol with the glycerol backbone.[151] In these studies[150–152] the responses of the glycerol backbone and choline headgroup to increasing cholesterol content were not, however, compared to experiments.

Fig. 9 shows the responses of the choline headgroup (β and α) order parameters of POPC (measured by ^{1}H-^{13}C NMR[35]) and DPPC (^{2}H NMR[47]) to increasing cholesterol content. Again, the two independent data sets agree very well: Only very modest ($\Delta S_{\mathrm{CH}} < 0.03$) changes occur in the choline order parameters as cholesterol content increases from 0 to 60%. The extreme sensitivity of the high resolution ^{2}H NMR experiments is beautifully demonstrated by the measurable[47] (but barely visible on the scale used in Fig. 9) cholesterol-induced forking of the α order parameter.

We note that the modest ($\Delta S_{\mathrm{CH}} < 0.02$ for g_1; < 0.04 for g_2, g_3; see Fig. 9) effects of cholesterol on the glycerol backbone order parameters of POPC measured by ^{1}H-^{13}C NMR[35] agree well with the results for phosphatidylethanolamine (PE) measured by ^{2}H NMR.[156] This further supports the ideas that the glycerol backbone structural behaviour is independent of the headgroup composition[26] and that the headgroup structure is largely independent of the acyl chain region content unless charges are present.[27]

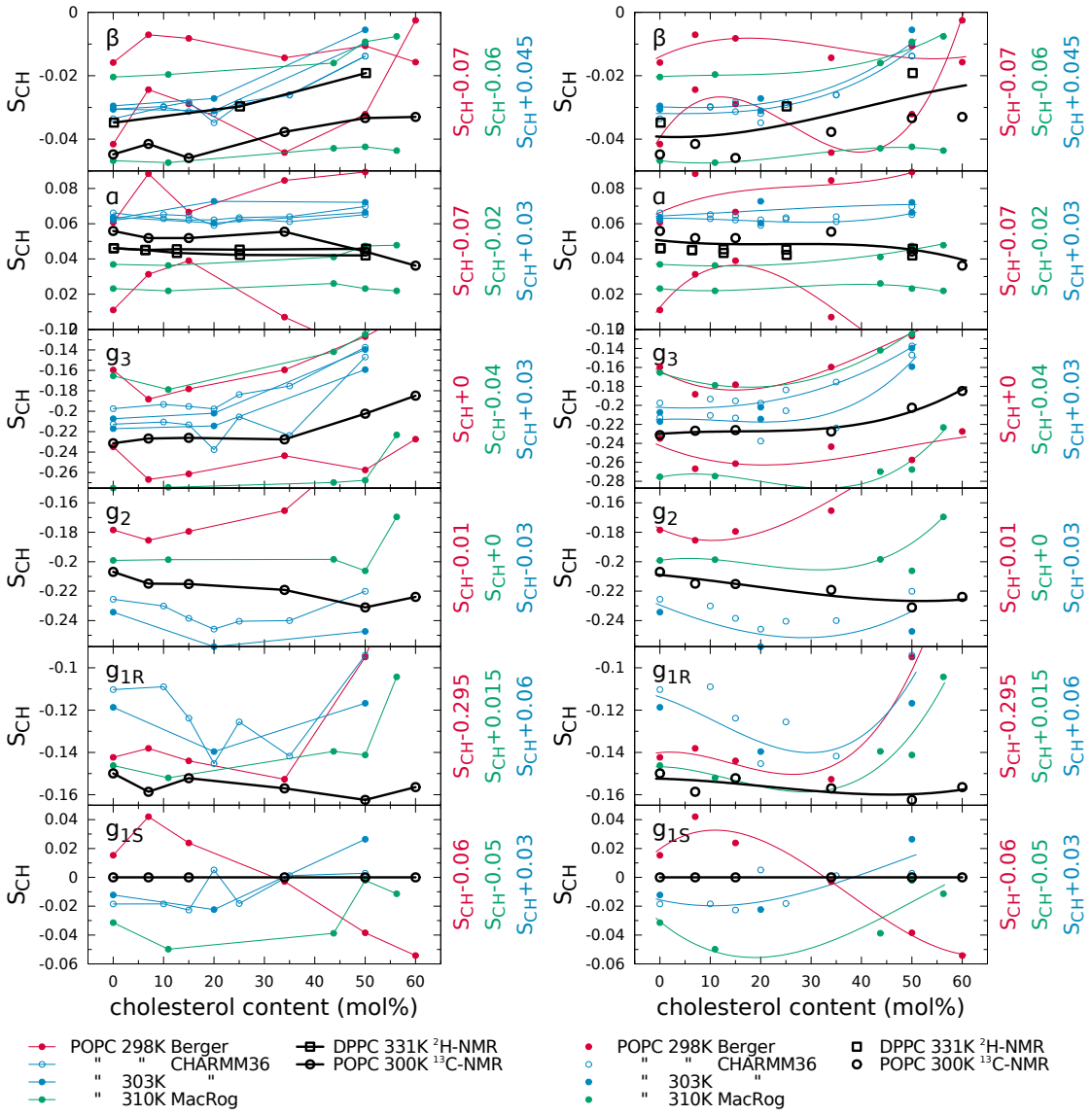

Figure 9: The effect of cholesterol content on the glycerol backbone and choline order parameters in experiments[35,47] and simulations with the Berger-POPC-07/Höltje-CHOL-13, CHARMM36 and MacRog force fields. The signs in the experimental values are based on the measurements by Hong et al.[16,65] and Gross et al.[66] Most order parameters from Berger-POPC-07/Höltje-CHOL-13 model for g_1 are beoynd the y-axis scale. In order to elucidate the relative change as a function of cholesterol content, the simulation results are shifted such that the (smaller) S_{CH} matches (within ± 0.01) the experimental value without cholesterol; the shift magnitudes for each of the force fields are listed (S_{CH}+shift) in the y-label.

3.Markus prepared two versions of this plot. The one on left has all the data points joint by lines; the one on right shows smooth trend lines (cubic polynomials) to ease qualitative comparison. Samuli likes the one on left, Markus the one on right. Do others have opinions?

In addition to the experimental data, Fig. 9 shows our results for the CHARMM36 and MacRog force fields and the previously published[35] Berger-POPC-07/Höltje-CHOL-13 results. Note that the simulation data are shifted vertically to ease comparison with experimental responses. As previously pointed out,[35] the Berger-based model seriously exaggerates the effect of cholesterol on the phospholipid glycerol backbone and choline headgroup. In comparison, the choline and glycerol backbone responses of CHARMM36 and MacRog are in better qualitative agreement with experiments. Therefore, to resolve the nature of cholesterol-induced structural changes, we calculated from CHARMM36 the glycerol backbone dihedral angle distributions at various cholesterol contents (Supplementary material): The only detectable change is the small decrease of gauche(-) and increase of gaughe(+) probability of the g_3-g_2-g_1-O(*sn*-1) dihedral. In conclusion, our results suggest that the significant effects of cholesterol on lipid conformations observed in simulations[150–152] are overestimated by the computational models used; cholesterol only induces very small structural changes in the glycerol backbone.

Finally, it is important to note that the CHARMM36 force field parameters (glycerol backbone dihedral potentials) have been tuned to reproduce the experimental order parameters at full hydration.[31] This approach introduces a risk of overfitting, which would manifest itself as wrong responses to changing conditions. Interestingly, according to our results, tuning did not lead to overfitting problems as far as dehydration or cholesterol content are considered.

Conclusions

The atomistic resolution structures sampled by the glycerol backbone and choline headgroup in phoshatidylcholine bilayers are not known despite of vast amount of accurate experimental data. An atomistic resolution molecular dynamics simulation model that would reproduce the experimental data would automatically resolve the structures, thus giving an unprecedently detailed interpretation of the experimental data. In this work we have collected and reviewed the experimental C–H bond vector order parameters available in the literature. These accurate experimental data are then compared to 13 different atomistic resolution simulation models for a fully hydrated lipid bilayer system, followed by bilayers dehydrated to different extents, and finally bilayers containing various amounts of cholesterol. We are led to the following four main conclusions:

(1) The C–H bond order parameters measured with different NMR techniques are consistent. By combining the experimental results from various sources we concluded that the order parameters for each C–H bond are known with a quantitative accuracy of ± 0.02.

(2) Comparison of order parameters between experiments and different atomistic resolution models together with structural analysis showed that the order parameters can be used to judge the structural accuracy of a model. Thus the combination of atomistic resolution molecular dynamics simulations and NMR experiments can be used to resolve the atomistic resolution structures of biomolecules in biologically relevant conditions. This approach can be extended from lipids to, for example, membrane proteins.

(3) The review of previous experimental results revealed that when a bilayer is dehydrated the choline order parameters increase. Our simulations suggested that this can be explained by the P–N vector tilting more parallel to the membrane. This strongly supports and complements the idea that charge-induced choline tilting can be measured using order parameter changes.[54,59]

(4) Only modest changes of glycerol backbone and choline order parameters are observed experimentally with increasing cholesterol content. When interpreted using the computa-

tional lipid model that we found to have the most realistic response to cholesterol, this observation means that cholesterol induces only minor changes in (the g_3-g_2-g_1-O(sn-1) dihedral of the glycerol backbone, in other words, there is no major conformational change of the lipid.

(+) Besides these four main conclusions, we note that we have created the most extensive publicly available collection of molecular dynamics simulation trajectories of lipid bilayers (`https://zenodo.org/collection/user-nmrlipids`). The mere existence of this collection opens up numerous possibilities for unforeseen analyses, such as data mining, and rapid testing of ideas with much less computational effort than previously required.

In general, we conclude that in order to fully utilize the potential of atomistic-resolution classical molecular dynamics simulations in the structural interpretation of high resolution NMR data[157] for lipid bilayers, one must improve the phoshatidylcholine glycerol backbone and choline headgroup parameters of the existing force fields.

This work has been done as a fully open collaboration, using `nmrlipids.blogspot.fi` as the communication platform. All the scientific contributions have been communicated publicly through this blog.[60]

Acknowledgement

AB and CL acknowledges financial support from the French National Research Agency (ANR: Biolubrication by phospholipid membranes Bioub2012) and computing time allocation from Pôle Scientifique de Modélisation Numérique from the ENS Lyon (PSMN), and Centre Informatique National de l'Enseignement Supérieur (CINES, Montpelier, France) (Project c2015096850). FFR acknowledges CONACYT and DGAPA UNAM IG100513 for financial support, Cluster Híbrido de Supercómputo Xiuhcoatl - CINVESTAV and Miztli - UNAM for computational resources. MJ and JT acknowledge and CSC - IT Center for Science for computational resources (project number tty3979). MJ also acknowledges the Finnish Doctoral Programme in Computational Sciences (FICS) for funding. JT, MJ,

TR and WK acknowledge the funding from the Academy of Finland (Centre of Excellence program) and the European Research Council (Advanced Grant project CROWDED-PRO-LIPIDS). WK acknowledges CSC – IT Centre for Science (Espoo, Finland) for excellent computational resources (project number tty3995). MSM acknowledges financial support from the Volkswagen Foundation (86110). LM acknowledges funding proved by the Institut national de la santé et de la recherche médicale (INSERM). JM acknowledges CSC – IT Center for Science for computational resources. OHSO acknowledges Tiago Ferreira and Paavo Kinnunen for useful discussions, the Emil Aaltonen foundation for financial support, Aalto Science – IT project and CSC – IT Center for Science for computational resources. HS acknowleges Catherine Etchebest and Stéphane Téletchéa for useful discussions and continued support, the HPC resources granted from GENCI-CINES (Grant 2014-c2014077209) and computer facilities provided by Région Ile de France and INTS (SESAME 2009 project).

Supporting Information Available

Simulation details, one figure and author contributions.

This material is available free of charge via the Internet at `http://pubs.acs.org/`.

SUPPLEMENTARY INFORMATION

Simulation details

Berger based models

For the Berger based models we use here the following naming convention: Berger - {*molecule name*} - {*year when model published first time*} {*citation*}. The reason is that there are several different molecular topologies which are using the non-bonded parameters originally developed by Berger et al.[43] Thus the common factor in the Berger based models are the non-bonded parameters, while the molecule specific parameters might somewhat vary. However, the majority of the molecular level topologies are relying (especially for the glycerol backbone and headgroup) on the parameters originally introduced by Marrink et al.[81] This is the case for all the Berger based simulations discussed in this work.

POPC simulations at full hydration at 298 K and simulations studying the effect of cholesterol are the same as in previous publications.[35,73] In these simulation the POPC parameters introduced by Ollila et al[72] are used, which are using the non-bonded parameters of Berger[43] and a molecular topology from Tieleman et al.[158] with improved double bond dihedrals by Bachar et al.[159] Thus they are called Berger-POPC-07.[72] The cholesterol model is based on the parameters by Höltje et al.[129] with the exception that the atom types were changed from CH2/CH3 to LP2/LP3 to avoid overcondensation of the bilayer as suggested in ref.[160] Since this modification was introduced by Ferreira et al.,[35] we call the used cholesterol model as Höltje-CHOL-13.[35]

For the POPC at 323 K and POPC in low hydration the same force field parameters are used. For DPPC the implementation of Berger parameters[43] by Peter Tieleman et al. are used.[81] For all of these simulations a timestep of 2 fs was used with a leapfrog integrator. Covalent bond lengths were constrained with the LINCS algorithm.[161,162] Coordinates were written every 10 ps. PME[163,164] with real space cut-off of 1.0 nm was used for electrostatics. Plain cut-off was used for the Lennard-Jones interactions with a 1.0 nm cut-off. The

neighbor lists with cut-off of 1.0 nm were updated every 5 steps. Temperature was coupled separately for lipids and water to 298 K using the velocity-rescale method[165] with coupling constant 0.1 ps. Pressure was semi-isotropically coupled to the atmospheric pressure with the Berendsen method.[166]

CHARMM36

DPPC and POPC with 72 lipids. The starting structures in PDB format were downloaded from the NIH/NHLBI Laboratory of Computational Biology Membrane Biophysics Section website (`http://www.lobos.nih.gov/mbs/coords.shtml`), which refers to these as the final structures (for DPPC after 40 ns, POPC after 35 ns) of the NPT lipid bilayer trajectories used in the original CHARMM36 publication.[31] The TIP3P[167] water model was used to solvate the system. The publicly available CHARMM36 parameters in Gromacs format (September 2013 update: `charmm36_gmx_format_sep13.tgz`) from the MacKerell Lab website (`http://mackerell.umaryland.edu/CHARMM_ff_params.html`) were used. Timestep of 1 fs was used with the leapfrog integrator. Covalent bonds with hydrogens were constrained with LINCS algorithm.[161,162] Coordinates were written every 5 ps. PME[163,164] with real space cut-off of 1.4 nm was used for electrostatics. Lennard-Jones interactions were switched to zero between 0.8 nm and 1.2 nm. The neighbour lists with a cut-off of 1.4 nm were updated every 5 steps. Temperature was coupled separately for lipids and water to 303 K using the velocity-rescale method[165] with coupling constant of 0.2 ps. Pressure was semi-isotropically coupled to the atmospheric pressure with the Berendsen method.[166]

POPC with 128 lipids The starting structures for the pure POPC simulations was taken from the Slipids[100] website (`http://mmkluster.fos.su.se/slipids/Downloads.html`). The starting structures for mixed POPC/Cholesterol simulations were constructed with the CHARMM-GUI website.[168] They contained 100 POPC/24 cholesterol molecules and 80 POPC/80 cholesterol molecules for the simulations of 20% cholesterol and 50% cholesterol respectively. The TIP3P water model[167] was used to solvate the system. The pub-

licly available CHARMM36 forcefield parameters (`http://www.gromacs.org/@api/deki/files/184/=charmm36.ff\\\_4.5.4\_ref.tgz`) by Piggot et al.[6] were used. Cholesterol parameters came from Lim et al.[135] and were converted into GROMACS format with the PyTopol tool.[169] Single point energy calculation was done to assess the conversion. Simulations were performed for 200 ns and the last 100 ns was used for the calculations. Timestep of 2 fs was used with leapfrog integrator. All bond lengths were constrained with LINCS.[161,162] Temperature was maintened at 303 K with the velocity-rescale method[165] and a time constant of 0.2 ps. Pressure was maintained semiisotropically at 1 bar using the Parrinello–Rahman algorithm[170] with a time constant of 1.0 ps. The neighbour list with a cut-off of 1.2 nm was updated every 10 steps. Lennard-Jones interactions were switched to zero between 0.8 nm and 1.2 nm. PME[163,164] with real space cut-off of 1.2 nm was used for electrostatics.

POPC with 512 lipids. POPC The starting structures for simulations were constructed with the CHARMM-GUI website.[168] 512 POPC lipids (256 per leafleat) were used for the initial 0% concentration and they were subsequently substituted by cholesterol molecules to fulfil the desired concentration. The TIP3P[167] water model was used to solvate the system. The publicly available port of the CHARMM36 forcefield parameters (`mackerell.umaryland.edu/CHARMM_ff_params.html`) was used for both POPC and cholesterol. Simulations were performed for 170 ns and the last 100 ns was used for the calculations. Timestep of 1 fs was used with the leapfrog integrator. Covalent bonds with hydrogen were constrained with LINCS algorithm. Coordinates were written every 10 ps. PME with real space cut-off of 1.2 nm was used for electrostatics. Lennard-Jones interactions were switched to zero between 0.8 nm and 1.2 nm. The neighbour lists with a cut-off of 1.2 nm were updated every 5 steps. Temperature was coupled separately for cholesterol, lipids and water to 298 K using the velocity-rescale method with coupling constant of 0.2 ps. Pressure was semi-isotropically coupled to the atmospheric pressure with the Berendsen method.

MacRog

The lipid force field parameters were obtained from the developers and the parameters are presented in Refs. 37,87. A bilayer with 288 POPC lipids was hydrated with 12600 TIP3P water[167] molecules (∼44/lipid) and simulated for 100 ns with a time step of 2 fs. Data was saved every 10 ps and the first 20 ns of the trajectory was discarded from the analysis. All bond lengths were constrained with LINCS.[161,162] The temperatures of the lipids and the solvent were separately coupled to the Nosé–Hoover thermostat[171,172] with a target temperature of 310 K and a time constant of 0.4 ps. Semi-isotropical pressure coupling to 1 bar was obtained with the Parrinello–Rahman barostat[170] with a time constant of 1 ps. PME[163,164] was employed to calculate the long-range electrostatic interactions. Lennard-Jones interactions were cut off at 1 nm and the dispersion correction was applied to both energy and pressure. A neighbour list with a radius of 1 nm was updated every step.

Identical parameters were employed for both full hydration and for the dehydration simulations. The dehydration simulations were also run for 100 ns with data saved every 10 ps.

The initial structures for the simulations with 10, 40, 50 and 60 mol% of cholesterol were obtained by replacing 14, 56, 64 or 72 POPC molecules with cholesterol molecules in the initial structure containing 128 POPC molecules. These systems were simulated for 400 ns and the first 200 ns was discarded from analysis. Data was saved every 100 ps.

GAFFLipid

The initial structure in Lipidbook[173] had different glycerol backbone isomers in different leaflets. To generate the initial structure we took the structure delivered by Slipids developers.[100] Also this structure had one lipid with different glycerol backbone isomer. This lipid and one lipid from opposite leaflet were removed after the system was equilibrated.

The force field parameters were generated using files obtained from the Lipidbook website (`http://lipidbook.bioch.ox.ac.uk/package/show/id/150.html`).[173] The conversion to GROMACS compatible formats was performed using the acpype tool.[174] The accuracy of

the conversion was checked by calculating the total energy of a single POPC lipid molecule using the sander program which is part of the AmberTools14 package[175] and version 4.6.5 of GROMACS. A difference of 0.002 kcal/mol was obtained between the two programs.

Timestep of 2 fs was used in Langevin dynamics with zero friction term and collision frequency of 1.0 ps^{-1}. Covalent bonds with hydrogens were constrained with the LINCS algorithm.[161,162] Coordinates were written every 10 ps. PME[163,164] with a real space cut-off at 1.0 nm was used for electrostatics. Plain cut-off with 1 nm was used for Lennard-Jones interactions. The neighbour lists with a cut-off of 1.0 nm were updated every 5 steps. Pressure was semi-isotropically coupled to a pressure of 1 bar with the Berendsen method.[166]

It should be noted that the area per molecule with these settings for the GAFFlipid model was 61.6 $Å^2$, while the original publication reported 63.9 $Å^2$.[33] However, the same parameters and Amber to Gromacs conversion reproduced the area per molecule from original publication for the lipid14 model (see next section).

Lipid14

The initial structure was taken directly from the Lipidbook.[173] The Amber compatible force field parameters were generated using the tleap program which is integrated in the AmberTools14 package.[175] A workflow similar to the one used previously for the conversion and validation of the GAFFLipid parameters was followed here. As before, a negligible energy difference of 0.003 kcal/mol was obtained between the two programs.

Timestep of 2 fs was used in Langevin dynamics with zero friction term and collision frequency of 1.0 ps^{-1}. Covalent bonds with hydrogens were constrained with LINCS algorithm.[161,162] Coordinates were written every 10 ps. PME[163,164] with real space cut-off of 1.0 nm was used for electrostatics. Plain cut-off with 1 nm was used for Lennard-Jones interactions. Dispersion correction was applied for both energy and pressure. The neighbor lists with a cut-off of 1.0 nm were updated every 5 steps. Pressure was semi-isotropically coupled to a pressure of 1 bar with the Berendsen method.[166]

The area per molecule with these settings was 65.4 Å^2 which is in agreement with the value reported in the original publication 65.6±0.5 Å^2.[93]

Poger et al.

The Poger lipids are derived from GROMOS G53A6[95] and were initially coined 53A6-L (L for lipids). They are now part of GROMOS G54A7[34] and parametrized to work with the SPC water model.[176] The initial hydrated bilayer structure of 128 DPPC and 5841 water molecules as well as force field parameters were downloaded from David Poger's web site (`http://compbio.chemistry.uq.edu.au/~david/`) on April 2012. We noticed that the same files downloaded in October 2013 appear to lack two dihedral angles in the choline headgroup (only one dihedral of type gd_29 allowing the rotation of the 3 choline methyls) compared to the April 2012 version (3 dihedrals of type gd_29 for the 3 choline methyls). This should not affect the bilayer structure and only change the kinetics of the choline methyls rotation. However the October 2013 version has not been tested in this study.

MD Simulations (two repetitions with independent initial velocities) were run for 100 ns using a 2 fs time step and the analysis was performed on the last 50 ns. Coordinates were saved every 50 ps for analysis. All bond lengths were constrained with the LINCS algorithm.[161,162] Temperature was kept at 323 K employing the velocity-rescale[165] thermostat with a time constant of 0.1 ps (DPPC and water coupled separetly). Pressure was maintained semi-isotropically at 1 bar using the Parrinello–Rahman barostat[170] using a 4 ps time constant and a compressibility of 4.5e-5 bar^{-1}. For non-bonded interactions, two conditions were tested: i) A 0.8–1.4 nm twin-range cut-off with the neighbor list updated every 5 steps for both electrostatics and Lennard-Jones (LJ) interactions (simulation files available at[177,178]). For the former the generalized reaction field (RF) with a dielectric permittivity of 62 was used beyond the 1.4 nm cut-off.[179] This is the original setup that Poger et al.[95] used. ii) PME[163,164] electrostatics with a real space cut-off of 1.0 nm, a Fourier spacing of 0.12 nm and an interpolation order of 4, LJ interactions computed with a 1.0–1.4 nm twin-range cut-

off, neighbor list updated every 5 steps (simulation files available at[96,97]). Note that Poger and Mark tested the effect of PME vs RF in ref.,[34] but used a 1.0 nm cut-off with PME and 1.4 nm with RF for LJ interactions. Since 0.8–1.4 nm twin-range cut-off for LJ interations is used in the parametrization of GROMOS force field, we decided to use that also in the simulations with PME.

Since Poger lipids come from the GROMOS force field, it is important to note that GROMOS uses the RF scheme for computing electrostatics (this is the method used for the force field parameterization). Using setup i) based on RF, we were able to reproduce the results (i.e. area per lipid value of 0.63 nm^2) from the original work only with GROMACS versions 4.0.X and earlier (the original authors[95] used GROMACS version 3.3.3). When switching to versions 4.5.X and above, the area per lipid dropped to below 0.58 nm^2. The GROMACS developers were contacted and a redmine issue opened (`http://redmine.gromacs.org/issues/1400`). The difference comes from the new Trotter decomposition introduced in versions 4.5.X. A fix has been introduced in version 4.6.6 that allows a recovery of an area per lipid value of 0.615 nm^2. The results in terms of area per lipid using the different GROMACS versions are available at.[178] Thus we decided to use only the PME setup ii) for computing the order parameter since it gives stable results regardless of the GROMACS version. We obtained an area per lipid of 0.615 nm^2, below 0.648 nm^2 found by the original authors with their PME setup (see[34]). We explained that by the fact that we used a 1.4 nm for the LJ cut-off whereas a value of 1.0 nm was used in the original publication.

Slipids

Initial coordinates for a hydrated DPPC (at 323 K) and POPC (at 310 K) bilayers (30 and 40 waters/lipid, respectively) were taken directly from the Slipids home page `http://mmkluster.fos.su.se/slipids/Downloads.html`. The Slipids force field[98,100] was used for the the all atom descriptions of DPPC and POPC, and water was described with the

TIP3P water model.[167] Simulations were performed within the NPT ensemble using the GROMACS 4.6.X simulation package.[74] The Nosé–Hoover thermostat[171,172] was used with reference temperatures of 323 K (DPPC) and 310 K (POPC) and a relaxation time constant of 0.5 ps. Water and lipids were coupled separately to the heat bath. Pressure was kept constant at 1.013 bar using a semi–isotropic Parrinello–Rahman barostat[170] with a time constant of 10.0 ps. Equations of motion were integrated with the leapfrog algorithm using a timestep of 2 fs. Long range electrostatic interactions were calculated using the PME method,[163,164] with a fourth order smoothing spline. A real space cut-off of 1.0 nm was employed with grid spacing of 0.12 nm in the reciprocal space. Lennard-Jones potentials were cut off at 1.4 nm, with a dispersion correction applied to both energy and pressure. All covalent bonds in lipids were constrained using the LINCS algorithm,[161] whereas water molecules were constrained using SETTLE.[180] Twin-range cutoffs, 1.0 nm and 1.6 nm, were used for the neighbor lists with the longrange neighbor list updated every 10 steps. This simulation protocol corresponds to the protocol used in Ref.[181]

Kukol

A bilayer patch with 512 POPC lipids was constructed and hydrated with ∼40 SPC water molecules per lipid. The force field parameters were obtained from Lipidbook.[173] This bilayer was simulated with a 2 fs time step for a total of 50 ns and coordinates were saved every 100 ps. All bonds were constrained with LINCS.[161,162] PME[163,164] was employed for the long-range electrostatics. Lennard-Jones interactions were cut off at 1.4 nm. A neighbour list with a radius of 0.8 nm was updated every 5 steps. The constant temperature of 298 K was maintained with the Berendsen thermostat[166] with a time constant of 0.1 ps. The Berendsen barostat[166] was employed for semi-isotropical pressure coupling at 1 bar.

Chiu et al.

The force field parameters and the initial configuration were available through the Lipidbook.[173] Timestep of 2 fs was used with leapfrog integrator. Covalent bond lengths were constrained with LINCS algorithm.[161,162] Coordinates were written every 10 ps. PME[163,164] with real space cut-off of 1.0 nm was used for electrostatics. Twin range cut-off was used for the Lennard-Jones interactions with short and long cut-offs of 1.0 nm and 1.6 nm, respectively. The neighbour lists with a cut-off of 1.0 nm were updated every 5 steps. Temperature was coupled separately for lipids and water to 298 K with the velocity-rescale method[165] with a coupling constant 0.2 ps. Pressure was semi-isotropically coupled to the atmospheric pressure with the Parrinello–Rahman method.[170]

Ulmschneider

The initial structure containing 128 POPC molecules with 3328 TIP3P water[167] molecules (26 per lipid) was downloaded from Lipidbook[173] together with the topologies. This bilayer was simulated for 100 ns with a time step of 2 fs and the data was saved every 10 ps. The bonds involving hydrogen atoms were constrained with LINCS.[161,162] The temperature was kept at 298 K with the Berendsen thermostat.[166] The pressure was semi-isotropically coupled to the Berendsen barostat[166] with a time constant of 1 ps and a target pressure of 1 bar. PME[163,164] was employed for long range electrostatics and a cut-off of 1 ns was employed for the Lennard-Jones interactions. A neighbour list with a radius of 1 nm was updated every 10 steps.

Additionally, the simulations were repeated with the dispersion correction applied to pressure and temperature. Even though the area per lipid decrease d slightly, the headgroup order parameters were only slightly affected.

Tjörnhammar et al.

The gel phase DPPC bilayer structure delivered by Tjörnhammar and Edholm[111] was ran for 5 ns at 343 K in order to destroy the ordered gel configuration. This was followed by a 200 ns simulation at 323 K, i.e. in the fluid phase. The last 100 ns of this simulation was used for analysis. The same mdp file as in the Supplementary Information section of the original paper [111] was used except for the simulation temperature.

Lee-CHARMM36-UA

A hydrated bilayer consisting of 72 DLPC lipids and 2189 water molecules is constructed using the model by Lee et al. [115] This model describes the important all-atom CHARMM36 character of the lipid headgroup but reduces the details of the lipid chains into a united-atom model. The initial equilibrated structure was downloaded from the web page of J. Klauda, Department of Chemical and Biomolecular Engineering University of Maryland. The parameter files are taken from the Supplementary Material of Ref. 115. This bilayer was equilibrated for 20 ns and the production run was 50 ns long, with data was saved every 20 ps. The equations of motion were integrated using the multiple time step Verlet r-RESPA algorithm with a time step of 2 fs, and a calculation of the electrostatic forces only every two timesteps. Covalent bonds between heavy and hydrogen atoms were constrained using SHAKE/RATTLE algorithm.[180]

The temperature was kept at 323 K with a Langevin thermostat with a damping coefficient of 5 ps. The modified NAMD version of the Nose-Hoover barostat with Langevin dynamics (piston period of 0.1 ps and piston decay time of 0.05 ps) was used semi-isotropically to reach the averaged target pressure of 1 bar and an averaged zero surface tension. PME[163,164] was employed for long range electrostatics. A cut-off of 1.2 nm was employed for the Lennard-Jones interactions, with a force-based switching function for distances beyond 1 nm. A neighbour list with a radius of 1.4 nm was updated every 10 timesteps.

NAMD was developed by the Theoretical and Computational Biophysics Group in the

Beckman Institute for Advanced Science and Technology at the University of Illinois at Urbana-Champaign.[77]

Botan-CHARMM36-UA

This model is similar to the Lee-CHARMM36-UA model with a few differences. A hydrated bilayer consisting of 128 DLPC lipids and 3840 water molecules is described by a model derived from the CHARMM27-UA model by Hénin et al.[113]

The distribution into all-atom (AA) and united-atom (UA) parts within the lipids is the same as in the original CHARMM27-UA model by Hénin et al.[113] This distribution differs from the one by Lee-CHARMM36-UA model solely for the first methylene groups of the two acyl chains (C22 and C32 in CHARMM36 topology): their hydrogens are merged into united atoms, whereas in Lee's model their hydrogens are described explicitely. The united-atom Berger model [43] was used for the tails and the UA-AA interactions as in Ref. 113. The difference between this model and the original one by Hénin[113] is the replacement of the AA parameters for the heads by the parameters of the all-atom CHARMM36 force-field.[31] Contrarily to the model by Lee et al.,[115] no reparametrization was done.

The non-bonded interactions are calculated using an atom-based switching function with short and long cut-offs of 0.8 and 1.2 nm. Long range electrostatic interactions are implemented using the particle-particle particle-mesh solver with a relative accuracy of 10^{-4}. The system is first equilibrated for 30 ns in the NPγT ensemble (Nosé–Hoover[171,172] style thermostat and barostat with anisotropic pressure coupling) at 323 K and 1 bar with timestep of 1 fs. The following 20 ns of dynamics are taken for calculation of configurational averages. Simulations were carried out by using the LAMMPS package.[75]

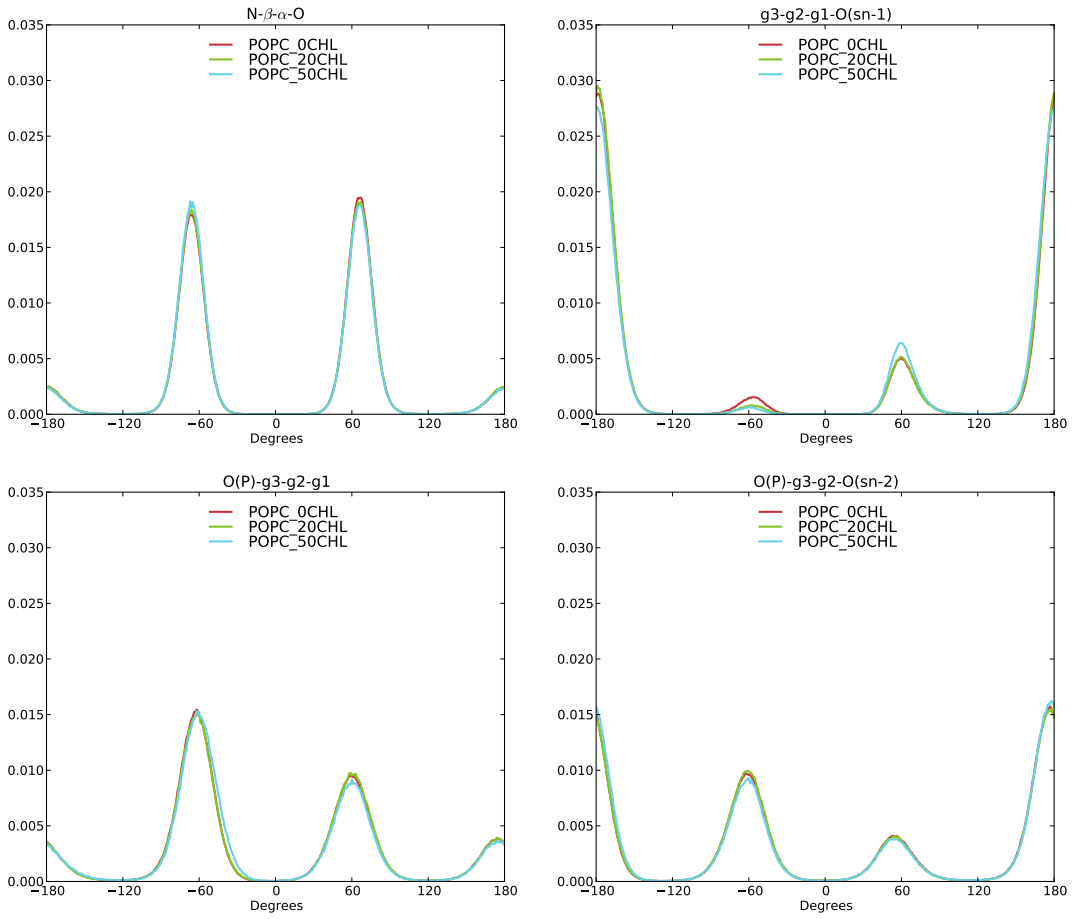

Figure 10: The effect of cholesterol content on the POPC glycerol backbone and choline dihedral angles in CHARMM36 model (T=303 K).

Dihedral angle distributions as a function of cholesterol in CHARMM36

Author Contributions

Alexandru Botan provided simulation results for charmm36-UA

Fernando Favela prepared, performed and analyzed simulations with popc and cholesterol for the CHARMM36 All-Atom FF.

Patrick F. J. Fuchs Ran and analyzed the Poger simulations. Provided scientific information which significantly advanced the project (signs and forking of order parameters).

Matti Javanainen prepared and performed simulations with multiple lipid models and analyzed the results. Supervised the work of JT.

Matej Kanduc provided simulation results for the Berger DLPC model

Waldemar Kulig prepared the MD simulations with cholesterol for the MacRog FF

Antti Lamberg Prepared and performed simulations with Berger and its variants to show the importance of the signs and stereospecific labeling of the order parameters.

Claire Loison provided simulation results for charmm36-UA.

Alexander Lyubartsev provided simulation results for Hgberg08 force field.

Markus S. Miettinen Co-designed the project with OHSO and supported in the work management. Provided trajectories for Berger DMPC; prepared parameter files for 72 lipids

Luca Monticelli Critical discussions in all phases of the project. Collaboration with Jukka Määttä.

Jukka Määttä prepared and performed simulations with Berger and Slipids models and analyzed the results.

*O. H. Samuli Ollila*Co-designed the project with MSM and managed the work. Ran and analyzed several simulations. Wrote the manuscript.

Marius Retegan Prepared and validated the GROMACS compatible parameter files for GAFFlipid and Lipid14 force fields.

Tomasz Rog Provided the topologies for the MacRog model and also the full hydration sim-

ulation data with this model.

Hubert Santuz prepared and performed the cholesterol simulations with CHARMM36 and analyzed the results. Made significant contribution in the data management of the project.

Joona Tynkkynen prepared and performed the dehydration simulations with the MacRog FF.

References

(1) Lipowsky, R., Sackmann, E., Eds. *Structure and Dynamics of Membranes*; Elsevier, 1995.

(2) Tieleman, D. P.; Marrink, S. J.; Berendsen, H. J. C. *Biochim. Biophys. Acta* **1997**, *1331*, 235–270.

(3) Klauda, J. B.; Venable, R. M.; Jr., A. D. M.; Pastor, R. W. In *Computational Modeling of Membrane Bilayers*; Feller, S. E., Ed.; Current Topics in Membranes; Academic Press, 2008; Vol. 60; pp 1 – 48.

(4) Edholm, O. In *Computational Modeling of Membrane Bilayers*; Feller, S. E., Ed.; Current Topics in Membranes; Academic Press, 2008; Vol. 60; pp 91 – 110.

(5) Tieleman, D. P. In *Molecular Simulations and Biomembranes: From Biophysics to Function*; Sansom, M., Biggin, P., Eds.; The Royal Society of Chemistry, 2010; pp 1–25.

(6) Piggot, T. J.; Piñeiro, Á.; Khalid, S. *J. Chem. Theory Comput.* **2012**, *8*, 4593–4609.

(7) Rabinovich, A.; Lyubartsev, A. *Polymer Science Series C* **2013**, *55*, 162–180.

(8) Marsh, D. *Handbook of Lipid Bilayers, Second Edition*; RSC press, 2013.

(9) Israelachvili, J. N.; Marcelja, S.; Horn, R. G. *Q. Rev. Biophys.* **1980**, *13*, 121–200.

(10) Seelig, J.; Gally, H.-U.; Wohlgemuth, R. *Biochim. Biophys. Acta* **1977**, *467*, 109 – 119.

(11) Skarjune, R.; Oldfield, E. *Biochemistry* **1979**, *18*, 5903–5909.

(12) Jacobs, R. E.; Oldfield, E. *Prog. Nucl. Mag. Res. Sp.* **1980**, *14*, 113 – 136.

(13) Davis, J. H. *Biochim. Biophys. Acta* **1983**, *737*, 117 – 171.

(14) Strenk, L.; Westerman, P.; Doane, J. *Biophys. J.* **1985**, *48*, 765 – 773.

(15) Akutsu, H.; Nagamori, T. *Biochemistry* **1991**, *30*, 4510–4516.

(16) Hong, M.; Schmidt-Rohr, K.; Nanz, D. *Biophys. J.* **1995**, *69*, 1939 – 1950.

(17) Hong, M.; Schmidt-Rohr, K.; Zimmermann, H. *Biochemistry* **1996**, *35*, 8335–8341.

(18) Semchyschyn, D. J.; Macdonald, P. M. *Magn. Res. Chem.* **2004**, *42*, 89–104.

(19) Hauser, H.; Guyer, W.; Pascher, I.; Skrabal, P.; Sundell, S. *Biochemistry* **1980**, *19*, 366–373.

(20) Hauser, H.; Guyer, W.; Paltauf, F. *Chem. Phys. Lipids* **1981**, *29*, 103 – 120.

(21) Hauser, H.; Pascher, I.; Pearson, R.; Sundell, S. *Biochim. Biophys. Acta* **1981**, *650*, 21 – 51.

(22) Akutsu, H. *Biochemistry* **1981**, *20*, 7359–7366.

(23) Pascher, I.; Lundmark, M.; Nyholm, P.-G.; Sundell, S. *Biochim. Biophys. Acta* **1992**, *1113*, 339 – 373.

(24) Hauser, H.; Pascher, I.; Sundell, S. *Biochemistry* **1988**, *27*, 9166–9174.

(25) Marsh, D.; Páli, T. *Chem. Phys. Lipids* **2006**, *141*, 48 – 65.

(26) Gally, H. U.; Pluschke, G.; Overath, P.; Seelig, J. *Biochemistry* **1981**, *20*, 1826–1831.

(27) Scherer, P.; Seelig, J. *The EMBO journal* **1987**, *6*.

(28) Shinoda, W.; Namiki, N.; Okazaki, S. *J. Chem. Phys.* **1997**, *106*, 5731–5743.

(29) Högberg, C.-J.; Nikitin, A. M.; Lyubartsev, A. P. *J. Comput. Chem.* **2008**, *29*, 2359–2369.

(30) Castro, V.; Stevensson, B.; Dvinskikh, S. V.; Högberg, C.-J.; Lyubartsev, A. P.; Zimmermann, H.; Sandström, D.; Maliniak, A. *Biochim. Biophys. Acta - Biomembranes* **2008**, *1778*, 2604 – 2611.

(31) Klauda, J. B.; Venable, R. M.; Freites, J. A.; O'Connor, J. W.; Tobias, D. J.; Mondragon-Ramirez, C.; Vorobyov, I.; Jr, A. D. M.; Pastor, R. W. *J. Phys. Chem. B* **2010**, *114*, 7830–7843.

(32) Kapla, J.; Stevensson, B.; Dahlberg, M.; Maliniak, A. *J. Phys. Chem. B* **2012**, *116*, 244–252.

(33) Dickson, C. J.; Rosso, L.; Betz, R. M.; Walker, R. C.; Gould, I. R. *Soft Matter* **2012**, *8*, 9617–9627.

(34) Poger, D.; Mark, A. E. *J. Chem. Theory Comput.* **2012**, *8*, 4807–4817.

(35) Ferreira, T. M.; Coreta-Gomes, F.; Ollila, O. H. S.; Moreno, M. J.; Vaz, W. L. C.; Topgaard, D. *Phys. Chem. Chem. Phys.* **2013**, *15*, 1976–1989.

(36) Chowdhary, J.; Harder, E.; Lopes, P. E. M.; Huang, L.; MacKerell, A. D.; Roux, B. *J. Phys. Chem. B* **2013**, *117*, 9142–9160.

(37) Maciejewski, A.; Pasenkiewicz-Gierula, M.; Cramariuc, O.; Vattulainen, I.; Rog, T. *J. Phys. Chem. B* **2014**, *118*, 4571–4581.

(38) Robinson, A.; Richards, W.; Thomas, P.; Hann, M. *Biophys. J.* **1994**, *67*, 2345 – 2354.

(39) Essex, J. W.; Hann, M. M.; Richards, W. G. *Philos. T. Roy. Soc. B* **1994**, *344*, 239–260.

(40) Kothekar, V. *Ind. J. Biochem. Biophys.* **1996**, *33*, 431 – 447.

(41) Hyvönen, M. T.; Rantala, T. T.; Ala-Korpela, M. *Biophys. J.* **1997**, *73*, 2907–2923.

(42) Duong, T. H.; Mehler, E. L.; Weinstein, H. *J. Comput. Phys.* **1999**, *151*, 358 – 387.

(43) Berger, O.; Edholm, O.; Jähnig, F. *Biophys. J.* **1997**, *72*, 2002 – 2013.

(44) Bechinger, B.; Seelig, J. *Chem. Phys. Lipids* **1991**, *58*, 1 – 5.

(45) Ulrich, A.; Watts, A. *Biophys. J.* **1994**, *66*, 1441 – 1449.

(46) Dvinskikh, S. V.; Castro, V.; Sandstrom, D. *Phys. Chem. Chem. Phys.* **2005**, *7*, 3255–3257.

(47) Brown, M. F.; Seelig, J. *Biochemistry* **1978**, *17*, 381–384.

(48) Brown, M. F.; Seelig, J. *Nature* **1977**, *269*, 721–723.

(49) Akutsu, H.; Seelig, J. *Biochemistry* **1981**, *20*, 7366–7373.

(50) Altenbach, C.; Seelig, J. *Biochemistry* **1984**, *23*, 3913–3920.

(51) Roux, M.; Bloom, M. *Biochemistry* **1990**, *29*, 7077–7089.

(52) Roux, M.; Bloom, M. *Biophys. J.* **1991**, *60*, 38 – 44.

(53) Gally, H. U.; Niederberger, W.; Seelig, J. *Biochemistry* **1975**, *14*, 3647–3652.

(54) Scherer, P. G.; Seelig, J. *Biochemistry* **1989**, *28*, 7720–7728.

(55) Browning, J. L.; Akutsu, H. *Biochim. Biophys. Acta* **1982**, *684*, 172 – 178.

(56) Kelusky, E. C.; Smith, I. C. *Mol. Pharmacol.* **1984**, *26*, 314–321.

(57) Roux, M.; Neumann, J. M.; Hodges, R. S.; Devaux, P. F.; Bloom, M. *Biochemistry* **1989**, *28*, 2313–2321.

(58) Kuchinka, E.; Seelig, J. *Biochemistry* **1989**, *28*, 4216–4221.

(59) Catte, A.; Javanainen, M.; Miettinen, M. S.; Oganesyan, V. S.; Ollila, O. H. S. Binding of cations to phospholipid bilayers. 2015; `https://www.dropbox.com/s/ebiwdsoj2otg4hp/LIPIDionINTERACT.pdf?dl=0`, Manuscript in preparation based on results in nmrlipids.blogspot.fi.

(60) The NMRLipids project. 2015; `http://web.archive.org/web/20150414084452/http://nmrlipids.blogspot.fi`.

(61) Gowers, T.; Nielsen, M. *Nature* **2009**, *461*, 879–881.

(62) Ollila, O. H. S. Response of the hydrophilic part of lipid membranes to changing conditions - a critical comparison of simulations to experiments. 2013; `http://arxiv.org/abs/1309.2131v1`.

(63) The NMRLipids project, On creadits. 2013; `http://web.archive.org/web/20150414092532/http://nmrlipids.blogspot.fi/2013/07/on-credits.html`.

(64) Seelig, J. *Q. Rev. Biophys.* **1977**, *10*, 353–418.

(65) Hong, M.; Schmidt-Rohr, K.; Pines, A. *J. Am. Chem. Soc.* **1995**, *117*, 3310–3311.

(66) Gross, J. D.; Warschawski, D. E.; Griffin, R. G. *J. Am. Chem. Soc.* **1997**, *119*, 796–802.

(67) Dvinskikh, S. V.; Castro, V.; Sandstrom, D. *Phys. Chem. Chem. Phys.* **2005**, *7*, 607–613.

(68) The NMRLipids project, Accuracy of order parameter measurements. 2014; http://web.archive.org/web/20150414085355/http://nmrlipids.blogspot.fi/2014/02/accuracy-of-order-parameter-measurements.html.

(69) The NMRLipids project, On the signs of the order parameters. 2014; http://web.archive.org/web/20150414085027/http://nmrlipids.blogspot.fi/2014/04/on-signs-of-order-parameters.html.

(70) Engel, A. K.; Cowburn, D. *FEBS Letters* **1981**, *126*, 169 – 171.

(71) Vogel, A.; Feller, S. *The Journal of Membrane Biology* **2012**, *245*, 23–28.

(72) Ollila, S.; Hyvönen, M. T.; Vattulainen, I. *J. Phys. Chem. B* **2007**, *111*, 3139–3150.

(73) Ferreira, T. M.; Ollila, O. H. S.; Pigliapochi, R.; Dabkowska, A. P.; Topgaard, D. *J. Chem. Phys.* **2015**, *142*, 044905.

(74) Hess, B.; Kutzner, C.; van der Spoel, D.; Lindahl, E. *J. Chem. Theory Comput.* **2008**, *4*, 435–447.

(75) Plimpton, S. *J. Comput. Phys.* **1995**, *117*, 1 – 19.

(76) Lyubartsev, A. P.; Laaksonen, A. *Comp. Phys. Comm.* **2000**, *128*, 565 – 589.

(77) Phillips, J. C.; Braun, R.; Wang, W.; Gumbart, J.; Tajkhorshid, E.; Villa, E.; Chipot, C.; Skeel, R. D.; Kalé, L.; Schulten, K. *J. Comput. Chem.* **2005**, *26*, 1781–1802.

(78) Gurtovenko, A. A.; Patra, M.; Karttunen, M.; Vattulainen, I. *Biophys. J.* **2004**, *86*, 3461 – 3472.

(79) Miettinen, M. S. Molecular dynamics simulation trajectory of a fully hydrated DMPC lipid bilayer. 2013; http://dx.doi.org/10.6084/m9.figshare.829642.

(80) Miettinen, M. S.; Gurtovenko, A. A.; Vattulainen, I.; Karttunen, M. *J. Phys. Chem. B* **2009**, *113*, 9226–9234.

(81) Marrink, S.-J.; Berger, O.; Tieleman, P.; Jähnig, F. *Biophys. J.* **1998**, *74*, 931 – 943.

(82) Määttä, J. DPPC_Berger. 2015; http://dx.doi.org/10.5281/zenodo.13934.

(83) Ollila, O. H. S.; Ferreira, T.; Topgaard, D. MD simulation trajectory and related files for POPC bilayer (Berger model delivered by Tieleman, Gromacs 4.5). 2014; http://dx.doi.org/10.5281/zenodo.13279.

(84) Samuli, O.; Markus, M. MD simulation trajectory and related files for DPPC bilayer (CHARMM36, Gromacs 4.5). 2015; http://dx.doi.org/10.5281/zenodo.15549.

(85) Samuli, O. O. H.; Miettinen, M. MD simulation trajectory and related files for POPC bilayer (CHARMM36, Gromacs 4.5). 2015; {http://dx.doi.org/10.5281/zenodo.13944}.

(86) Santuz, H. MD simulation trajectory and related files for POPC bilayer (CHARMM36, Gromacs 4.5). 2015; http://dx.doi.org/10.5281/zenodo.14066.

(87) Kulig, W.; Pasenkiewicz-Gierula, M.; Róg, T. Cis and Trans Unsaturated Phosphatidylcholine Bilayers: A Molecular Dynamics Simulation Study. 2015; Submitted.

(88) Javanainen, M. POPC @ 310K, model by Maciejewski and Rog. 2014; {http://dx.doi.org/10.5281/zenodo.13497}.

(89) Javanainen, M. POPC/Cholesterol @ 310K. 0, 10, 40, 50 and 60 mol-cholesterol. Model by Maciejewski and Rog. 2015; {http://dx.doi.org/10.5281/zenodo.13877}.

(90) Javanainen, M. POPC @ 310K, varying water-to-lipid ratio. Model by Maciejewski and Rog. 2014; {http://dx.doi.org/10.5281/zenodo.13498}.

(91) Samuli, O.; Retegan, M. MD simulation trajectory and related files for DPPC bilayer (GAFFlipid, Gromacs 4.5). 2015; http://dx.doi.org/10.5281/zenodo.15550.

(92) Ollila, O. H. S.; Retegan, M. MD simulation trajectory and related files for POPC bilayer (GAFFlipid, Gromacs 4.5). 2015; {http://dx.doi.org/10.5281/zenodo.13791}.

(93) Dickson, C. J.; Madej, B. D.; Skjevik, . A.; Betz, R. M.; Teigen, K.; Gould, I. R.; Walker, R. C. *J. Chem. Theory Comput.* **2014**, *10*, 865–879.

(94) Ollila, O. H. S.; Retegan, M. MD simulation trajectory and related files for POPC bilayer (Lipid14, Gromacs 4.5). 2014; http://dx.doi.org/10.5281/zenodo.12767.

(95) Poger, D.; Van Gunsteren, W. F.; Mark, A. E. *J. Comput. Chem.* **2010**, *31*, 1117–1125.

(96) Fuchs, P. F. MD simulation trajectory and related files for DPPC bilayer in full hydration (Poger GROMOS53A6_L, Gromacs 4.0.7, PME, traj 1). 2015; http://dx.doi.org/10.5281/zenodo.14594.

(97) Fuchs, P. F. MD simulation trajectory and related files for DPPC bilayer in full hydration (Poger GROMOS53A6_L, Gromacs 4.0.7, PME, traj 2). 2015; http://dx.doi.org/10.5281/zenodo.14595.

(98) Jämbeck, J. P. M.; Lyubartsev, A. P. *J. Phys. Chem. B* **2012**, *116*, 3164–3179.

(99) Määttä, J. DPPC_Slipids. 2014; {http://dx.doi.org/10.5281/zenodo.13287}.

(100) Jämbeck, J. P. M.; Lyubartsev, A. P. *J. Chem. Theory Comput.* **2012**, *8*, 2938–2948.

(101) Javanainen, M. POPC @ 310K, Slipids force field. 2015; http://dx.doi.org/10.5281/zenodo.13887.

(102) Kukol, A. *J. Chem. Theory Comput.* **2009**, *5*, 615–626.

(103) Javanainen, M. POPC @ 298K, Model by Kukol. 2014; {http://dx.doi.org/10.5281/zenodo.13393}.

(104) Chiu, S.-W.; Pandit, S. A.; Scott, H. L.; Jakobsson, E. *J. Phys. Chem. B* **2009**, *113*, 2748–2763.

(105) Samuli, O. MD simulation trajectory and related files for POPC bilayer (Chiu et al. Gromos version, Gromacs 4.5). 2015; http://dx.doi.org/10.5281/zenodo.15548.

(106) Lyubartsev, A. MD simulation trajectory and related files for DMPC bilayer, Högberg et al, J.Comp.Chem., 29, 2359 (2008). 2015; http://dx.doi.org/10.5281/zenodo.16195.

(107) Rabinovich, A. L.; Lyubartsev, A. P. *J. Phys. Conf. Ser.* **2014**, *510*, 012022.

(108) Lyubartsev, A. MD simulation trajectory and related files for POPC bilayer, Högberg et al parameters (J.Comp.Chem., 29, 2359 (2008)). 2015; http://dx.doi.org/10.5281/zenodo.16724.

(109) Ulmschneider, J. P.; Ulmschneider, M. B. *J. Chem. Theory Comput.* **2009**, *5*, 1803–1813.

(110) Javanainen, M. POPC @ 310K, Model by Ulmschneider and Ulmschneider. 2014; {http://dx.doi.org/10.5281/zenodo.13392}.

(111) Tjörnhammar, R.; Edholm, O. *J. Chem. Theory Comput.* **2014**, *10*, 5706–5715.

(112) Javanainen, M. DPPC @ 323K, new FF by Tjörnhammar and Edholm. 2014; http://dx.doi.org/10.5281/zenodo.12743.

(113) Henin, J.; Shinoda, W.; Klein, M. L. *J. Phys. Chem. B* **2008**, *112*, 7008–7015.

(114) Botan, A. DLPC@ 323K, CHARMM36UA force field. 2015; {http://dx.doi.org/10.5281/zenodo.13821}.

(115) Lee, S.; Tran, A.; Allsopp, M.; Lim, J. B.; Henin, J.; Klauda, J. B. *J. Phys. Chem. B* **2014**, *118*, 547–556.

(116) Loison, C. Hydrated DPPC, MD simulation trajectory and related files for UA charmm36 model by Lee et al 2014. 2015; http://dx.doi.org/10.5281/zenodo.17004.

(117) Ollila, O. H. S. MD simulation trajectory and related files for POPC bilayer in low hydration (Berger model delivered by Tieleman, Gromacs 4.5). 2015; {http://dx.doi.org/10.5281/zenodo.13814}.

(118) Kanduc, M.; Schneck, E.; Netz, R. R. *Langmuir* **2013**, *29*, 9126–9137.

(119) Kanduc, M. MD trajectory for DLPC bilayer (Berger, Gromacs 4.5.4), nw=28 w/l. 2015; http://dx.doi.org/10.5281/zenodo.16287.

(120) Kanduc, M. MD trajectory for DLPC bilayer (Berger, Gromacs 4.5.4), nw=24 w/l. 2015; http://dx.doi.org/10.5281/zenodo.16289.

(121) Kanduc, M. MD trajectory for DLPC bilayer (Berger, Gromacs 4.5.4), nw=20 w/l. 2015; http://dx.doi.org/10.5281/zenodo.16291.

(122) Kanduc, M. MD trajectory for DLPC bilayer (Berger, Gromacs 4.5.4), nw=16 w/l. 2015; http://dx.doi.org/10.5281/zenodo.16292.

(123) Kanduc, M. MD trajectory for DLPC bilayer (Berger, Gromacs 4.5.4), nw=28 w/l. 2015; http://dx.doi.org/10.5281/zenodo.16293.

(124) Kanduc, M. MD trajectory for DLPC bilayer (Berger, Gromacs 4.5.4), nw=8 w/l. 2015; http://dx.doi.org/10.5281/zenodo.16294.

(125) Kanduc, M. MD trajectory for DLPC bilayer (Berger, Gromacs 4.5.4), nw=4 w/l. 2015; http://dx.doi.org/10.5281/zenodo.16295.

(126) Samuli, O. O. H.; Miettinen, M. MD simulation trajectory and related files for POPC bilayer in medium low hydration (CHARMM36, Gromacs 4.5). 2015; {http://dx.doi.org/10.5281/zenodo.13946}.

(127) Samuli, O. O. H.; Miettinen, M. MD simulation trajectory and related files for POPC bilayer in low hydration (CHARMM36, Gromacs 4.5). 2015; {http://dx.doi.org/10.5281/zenodo.13945}.

(128) Ollila, O. H. S. MD simulation trajectory and related files for POPC bilayer in low hydration (GAFFlipid, Gromacs 4.5). 2015; {http://dx.doi.org/10.5281/zenodo.13853}.

(129) Höltje, M.; Förster, T.; Brandt, B.; Engels, T.; von Rybinski, W.; Höltje, H.-D. *Biochim. Biophys. Acta* **2001**, *1511*, 156 – 167.

(130) Ollila, O. H. S.; Ferreira, T.; Topgaard, D. MD simulation trajectory and related files for POPC/cholesterol (7 mol%) bilayer (Berger model delivered by Tieleman, modified Höltje, Gromacs 4.5). 2014; {http://dx.doi.org/10.5281/zenodo.13282}.

(131) Ollila, O. H. S.; Ferreira, T.; Topgaard, D. MD simulation trajectory and related files for POPC/cholesterol (15 mol%) bilayer (Berger model delivered by Tieleman, modified Höltje, Gromacs 4.5). 2014; {http://dx.doi.org/10.5281/zenodo.13281}.

(132) Ollila, O. H. S.; Ferreira, T.; Topgaard, D. MD simulation trajectory and related files for POPC/cholesterol (34 mol%) bilayer (Berger model delivered by Tieleman, modified Höltje, Gromacs 4.5). 2014; {http://dx.doi.org/10.5281/zenodo.13283}.

(133) Ollila, O. H. S.; Ferreira, T.; Topgaard, D. MD simulation trajectory and related files for POPC/cholesterol (50 mol%) bilayer (Berger model delivered by Tieleman, modified Höltje, Gromacs 4.5). 2014; {http://dx.doi.org/10.5281/zenodo.13285}.

(134) Ollila, O. H. S.; Ferreira, T.; Topgaard, D. MD simulation trajectory and related files for POPC/cholesterol (60 mol%) bilayer (Berger model delivered by Tieleman, modified Höltje, Gromacs 4.5). 2014; {http://dx.doi.org/10.5281/zenodo.13286}.

(135) Lim, J. B.; Rogaski, B.; Klauda, J. B. *J. Phys. Chem. B* **2012**, *116*, 203–210.

(136) Fernando, F.-R. POPC_Glycerol_CHARMM36_0-10-15-20-25-35-50%CHOL. 2015; http://dx.doi.org/10.5281/zenodo.16830, Because of the system size, the files ONLY contain the coordinates of Glycerol saved every 10ps, this is the real contribution to the nmrlipids project.

(137) Santuz, H. MD simulation trajectory for POPC/20% Chol bilayer (CHARMM36, Gromacs 4.5). 2015; http://dx.doi.org/10.5281/zenodo.14067.

(138) Santuz, H. MD simulation trajectory for POPC/50% Chol bilayer (CHARMM36, Gromacs 4.5). 2015; http://dx.doi.org/10.5281/zenodo.14068.

(139) Warschawski, D.; Devaux, P. *Eur. Biophys. J.* **2005**, *34*, 987–996.

(140) Mashl, R. J.; Scott, H. L.; Subramaniam, S.; Jakobsson, E. *Biophys. J.* **2001**, *81*, 3005 – 3015.

(141) Pertsin, A.; Platonov, D.; Grunze, M. *J. Chem. Phys.* **2005**, *122*, 244708.

(142) Pertsin, A.; Platonov, D.; Grunze, M. *Langmuir* **2007**, *23*, 1388–1393.

(143) Eun, C.; Berkowitz, M. L. *J. Phys. Chem. B* **2009**, *113*, 13222–13228.

(144) Eun, C.; Berkowitz, M. L. *J. Phys. Chem. B* **2010**, *114*, 3013–3019.

(145) Schneck, E.; Sedlmeier, F.; Netz, R. R. *Proc. Natl. Acad. Sci. USA* **2012**, *109*, 14405–14409.

(146) Israelachvili, J. N. *Intermolecular and Surface Forces*; Academic Press: London, 1985.

(147) Israelachvili, J. N.; Wennerström, H. *Nature* **1996**, *379*, 219 – 225.

(148) Sparr, E.; Wennerström, H. *Curr. Opin. Colloid Interf. Science* **2011**, *16*, 561 – 567.

(149) Huang, J.; Feigenson, G. W. *Biophys. J.* **1999**, *76*, 2142 – 2157.

(150) Zhu, Q.; Cheng, K. H.; Vaughn, M. W. *J. Phys. Chem. B* **2007**, *111*, 11021–11031.

(151) Rog, T.; Pasenkiewicz-Gierula, M.; Vattulainen, I.; Karttunen, M. *Biochim. Biophys. Acta* **2009**, *1788*, 97 – 121.

(152) Alwarawrah, M.; Dai, J.; Huang, J. *J. Chem. Theor. Comput.* **2012**, *8*, 749–758.

(153) Marsh, D. *Biochim. Biophys. Acta* **2010**, *1798*, 688 – 699.

(154) Simons, K.; Vaz, W. L. *Ann. Rev. Biophys. Biomol. Struct.* **2004**, *33*, 269–295.

(155) Somerharju, P.; Virtanen, J. A.; Cheng, K. H.; Hermansson, M. *Biochim. Biophys. Acta - Biomembranes* **2009**, *1788*, 12 – 23.

(156) Ghosh, R.; Seelig, J. *Biochim. Biophys. Acta* **1982**, *691*, 151 – 160.

(157) Ferreira, T. M.; Topgaard, D.; Ollila, O. H. S. *Langmuir* **2014**, *30*, 461–469.

(158) Tieleman, D. P.; Berendsen, H. J.; Sansom, M. S. *Biophys. J.* **1999**, *76*, 1757 – 1769.

(159) Bachar, M.; Brunelle, P.; Tieleman, D. P.; Rauk, A. *J. Phys. Chem. B* **2004**, *108*, 7170–7179.

(160) Tieleman, D. P.; MacCallum, J. L.; Ash, W. L.; Kandt, C.; Xu, Z.; Monticelli, L. *J. Phys. Condens. Matter* **2006**, *18*, S1221.

(161) Hess, B.; Bekker, H.; Berendsen, H. J. C.; Fraaije, J. G. E. M. *J. Comput. Chem.* **1997**, *18*, 1463–1472.

(162) Hess, B. *J. Chem. Theory Comput.* **2008**, *4*, 116–122.

(163) Darden, T.; York, D.; Pedersen, L. *J. Chem. Phys.* **1993**, *98*, 10089–10092.

(164) Essman, U. L.; Perera, M. L.; Berkowitz, M. L.; Larden, T.; Lee, H.; Pedersen, L. G. *J. Chem. Phys.* **1995**, *103*, 8577–8592.

(165) Bussi, G.; Donadio, D.; Parrinello, M. *J. Chem. Phys.* **2007**, *126*.

(166) Berendsen, H. J. C.; Postma, J. P. M.; van Gunsteren, W. F.; DiNola, A.; Haak, J. R. *J. Chem. Phys.* **1984**, *81*, 3684–3690.

(167) Jorgensen, W. L.; Chandrasekhar, J.; Madura, J. D.; Impey, R. W.; Klein, M. L. *J. Chem. Phys.* **1983**, *79*, 926–935.

(168) Jo, S.; Kim, T.; Iyer, V. G.; Im, W. *J. Comput. Chem.* **2008**, *29*, 1859–1865.

(169) Salari, R. PyTopol: A Library For Converting Molecular Topologies. 2015; `http://dx.doi.org/10.5281/zenodo.16084`.

(170) Parrinello, M.; Rahman, A. *J. Appl. Phys.* **1981**, *52*, 7182–7190.

(171) Nose, S. *Mol. Phys.* **1984**, *52*, 255–268.

(172) Hoover, W. G. *Phys. Rev. A* **1985**, *31*, 1695–1697.

(173) Domański, J.; Stansfeld, P.; Sansom, M.; Beckstein, O. *The Journal of Membrane Biology* **2010**, *236*, 255–258.

(174) Sousa da Silva, A.; Vranken, W. *BMC Research Notes* **2012**, *5*, 367.

(175) Salomon-Ferrer, R.; Case, D. A.; Walker, R. C. *Wiley Interdisciplinary Reviews: Computational Molecular Science* **2013**, *3*, 198–210.

(176) Berendsen, H. J. C.; Postma, J. P. M.; van Gunsteren, W. F.; Hermans, J. In *Intermolecular Forces*; Pullman, B., Ed.; Reidel: Dordrecht, 1981; Chapter Interaction models for water in relation to protein hydration, pp 331–342.

(177) Fuchs, P. F. MD simulation trajectory and related files for DPPC bilayer in full hydration (Poger GROMOS53A6_L, Gromacs 4.0.7, Reaction Field, traj 1). 2015; http://dx.doi.org/10.5281/zenodo.14592.

(178) Fuchs, P. F. MD simulation trajectory and related files for DPPC bilayer in full hydration (Poger GROMOS53A6_L, Gromacs 4.0.7, Reaction Field, traj 2). 2015; http://dx.doi.org/10.5281/zenodo.14591.

(179) Tironi, I. G.; Sperb, R.; Smith, P. E.; van Gunsteren, W. F. *J. Chem. Phys.* **1995**, *102*, 5451–5459.

(180) Miyamoto, S.; Kollman, P. A. *J. Comput. Chem* **1992**, *13*, 952–962.

(181) Jambeck, J. P. M.; Lyubartsev, A. P. *Phys. Chem. Chem. Phys.* **2013**, *15*, 4677–4686.

Graphical TOC Entry

Some journals require a graphical entry for the Table of Contents. This should be laid out "print ready" so that the sizing of the text is correct. Inside the `tocentry` environment, the font used is Helvetica 8 pt, as required by *Journal of the American Chemical Society*.
The surrounding frame is 9 cm by 3.5 cm, which is the maximum permitted for *Journal of the American Chemical Society* graphical table of content entries. The box will not resize if the content is too big: instead it will overflow the edge of the box.
This box and the associated title will always be printed on a separate page at the end of the document.